Androgen Producing Cells in Polycystic Ovaries

Margaret M. Convery

Department of Anatomy

McGill University

June 1989

A thesis submitted to the Faculty of Graduate Studies and Research
in partial fulfillment of the requirements
For the degree of Master of Science

ABSTRACT

A single injection of estradiol valerate (EV) produces a cascade of specific hypothalamic and pituitary impairments, culminating in polycystic ovaries (PCO) (macrocystic PCO). Chronic exposure to physiological levels of 17-ß-estradiol (E_2) via subcutaneous implants (Silastic R capsules) also results in a polycystic ovarian condition, about which less is known. The plasma gonadotropin patterns are very different in these two models, as is the histology of the polycystic ovaries. Since in both varieties of PCO thecal cells and thecal derivatives are very prominent, these cells have been studied at the light and electron microscopic level. Five indices of cytodifferentiation and steroid synthetic activity have been examined, including: alkaline phosphatase expression, LH binding capacity, mitochondrial area, lipid droplet area, and cell size.

Thecal cells from healthy and atretic follicles in both macrocystic and microcystic ovaries show intense alkaline phosphatase activity, numerous LH-binding sites, and the ultrastructural characteristics of cells active in steroidogenesis. Macrocystic and microcystic thecal cells express little alkaline phosphatase activity, possess a negligible number of LH binding sites, and contain the largest amount of lipid with respect to both the size of the droplets and abundance. These indices suggest that cystic thecal cells are steroidogenically inactive. Cystic follicles appear to be the result of an atretic process. In both the macrocystic and microcystic model, the process of atresia seems to involve a progressive deactivation of thecal cells, with cystic follicles representing the completion of the process. The large size of macrocystic follicles may prevent them from collapsing, and thus they remain in the ovary. Microcystic follicles, on the other hand, seem to be follicles in a terminal state of atresia, prior to collapse.

Secondary interstitial cell clusters in both macrocystic and microcystic ovaries show intense alkaline phosphatase activity and the largest number of LH-binding sites. This suggests that these cells are the most sensitive to tropic hormone stimulation, and the most actively androgenic. The ultrastructural characteristics of these cells, ie. mitochondrial and lipid droplet area, also suggest this. As the alkaline phosphatase

activity and number of LH binding sites between secondary interstitial cell clusters are more variable in EV-treated ovaries than in the E2-implanted model, and as E2-implanted ovaries contain a more extensive population of secondary interstitial cells, the androgen levels in the microcystic condition would be expected to be higher than in the macrocystic condition Differences between the EV-treated and E2-implanted polycystic ovaries may reflect differences in the pattern of tropic hormone stimulation.

Name: Margaret M. Convery

Title of Thesis: Androgen Producing Cells in Polycystic Ovaries

Department: Anatomy

Degree: Master of Science

Résumé

Une seule injection d'oestradiol valerate (EV) produit chez le rat une série de détériorations hypothalamiques et hypophysaires spécifiques qui culminent dans la formation d'ovaires polycystiques (PCO) (PCO macrocystique). Une exposition chronique à des niveaux physiologiques de 17-ß-oestradiol (E_2) via des implants sous-cutanés (capsules de polydiméthylsiloxane) a aussi pour résultat la formation d'ovaires polycystiques, condition sur laquelle on a moins d'information. Il y a une grande différence entre les profils du taux plasmatique des gonadotrophines ainsi que l'histologie des ovaires polycystiques de ces deux modèles. Comme les cellules thécales et leurs dérivées sont très proéminentes pour chaque type de PCO, ces cellules ont été étudiées en microscopie optique et électronique. Cinq indices de cytodifférentiation et d'activité synthétique des stéroïdes ont été examinés, incluant l'expression de la phosphatase alcaline, la capacité de liaison de LH, la superficie des mitochondries, la superficie des gouttelettes lipoïdes et la dimension des cellules.

Les cellules thécales provenant de follicules sains et atrésiques d'ovaires macrocystiques et microcystiques présentent une activité intense de la phosphatase alcaline, de nombreux sites de liaison de LH, et les caractéristiques ultrastructurales de cellules actives dans la production de stéroïdes. Les cellules thécales macrocystiques et microcystiques manifestent une faible activité de la phosphatase alcaline, possèdent un nombre négligeable de sites de liaison de LH et contiennent la plus grande quantité de lipide en ce qui concerne la dimension et l'abondance des gouttelettes. Ces indices suggèrent que ces cellules thécales cystiques sont inactives en ce qui a trait à la synthèse des stéroïdes. Les follicules cystiques semblent être le résultat d'un processus d'atrésie. Dans le cas du modèle macrocystique comme dans celui du modèle microcystique, le processus d'atrésie dont les follicules atrésiques représentent l'achèvement, semble impliquer un ralentissement progressif des cellules thécales. La grande dimension des follicules macrocystiques pourrait prévenir leur désagrégation et, par conséquent, ils restent dans l'ovaire. Par contre, les follicules microcystiques semblent être à un stage terminal d'atrésie avant leur désagrégation.

Les groupes secondaires de cellules interstitielles des ovaries macrocystiques et microcystiques présentent une activité intense de la phosphatase alcaline et le plus grand nombre de sites de liaison de LH Ceci suggère que ces cellules sont les plus sensibles a une stimulation hormonale trophique et les plus actives dans la formation d'androgenes. De même les caractéristiques ultrastructurales de ces cellules, ie. la superficie des mitochondries et des gouttelettes lipoïdes, suggèrent ceci. Comme l'activité de la phosphatase alcaline et le nombre de sites de liaison de LH entre les groupes secondaires de cellules interstitielles sont plus variables dans les ovaires traités à l'EV que dans le modèle implanté avec l'E_2, et comme les ovaires implantés avec l'E2 contiennent une population plus étendue de cellules secondaires interstitielles, on s'attend à ce que les niveaux d'androgènes de la condition microcystique soient plus élevés que ceux de la condition macrocystique. Les différences entre les ovaires traités à l'EV et ceux implantés avec l'E_2 pourraient refléter des différences dans le profil de stimulation des hormones trophiques.

Nom: Margaret M. Convery

Titre de la thèse: Les Cellules Qui Produisent L'androgène Dans Les Ovaires Polycystiques

Département: Anatomie

Diplôme: Maîtrise es Sciences

ACKNOWLEDGEMENTS

I wish to thank the following persons:

- Dr. James Brawer, for his supervision and guidance, his endless patience and encouragement, and for financial support.

- Dalia Piccioni-Chen, for her advice and technical assistance.

- Dr. Mike Lalli, Jeannie Mui, Pat Hales, Michael Kraetz, and all of the EM Lab technicians, for teaching me electron microscopic techniques and for their patience in helping me solve technical problems.

- Dr. Riaz Farookhi, for preparing the radioligand.

- Mr. A. Graham, for his assistance with photography.

- Len Wedlich, for his assistance in preparing the photographic figures.

- Michele Piotte, for translating the abstract for this thesis.

- The Center for the Study of Reproduction for their financial support.

- Grandma, for her emotional and financial support.

- Dad, Mom, Maureen, Michael, Kathleen, John, Sheila and Brian, for the countless phone calls and letters, and for their confidence and support.

I also wish to thank Jagjit Gill for his encouragement, his help, and for his friendship which has made the difficult days more bearable.

TABLE OF CONTENTS

INTRODUCTION

Cyclic reproductive function in mammals depends upon integrated interactions between the hypothalamus, the pituitary and the ovaries. Because the menstrual cycle (humans) and the estrous cycle (rodents) are true cycles, a first cause, ie. a cause without an antecedent cause, and a final end result cannot be identified. Cyclicity is dependent on the balanced reciprocal interaction between the brain, the pituitary and the ovaries. Alteration or loss of endocrine signals at any level along the hypothalamo-hypophyseal-gonadal axis leads to a disruption of the balance of the system, and a cessation of cyclicity and ovulation. A common consequence of such disruptions is Polycystic Ovarian Disease.

The polycystic ovarian condition (PCO) is a state of anovulatory acyclicity occurring in a wide range of mammalian species. This reproductive anomaly encompasses a range of expressions, and is not a single disease entity. The state of chronic anovulation is responsible for the infertility associated with PCO. PCO is a major cause of infertility in women, cattle, pork and sheep. It is characterized by the presence, within the ovaries, of multiple, large cystic follicles.

The anovulatory state of the ovaries in humans with PCO is presumably a response to the altered gonadotropin signals being released from the pituitary, (Yen et al., 1970). In our laboratory, we have generated chronic polycystic ovarian conditions in the rat by administering a single large dose of estradiol valerate (EV) (Brawer et al., 1978; Hemmings et al., 1983; Schulster et al., 1984), or by chronic

exposure to physiological levels of 17-β-estradiol from subcutaneously implanted silastic capsules (Brawer et al., 1983; Wilkinson et al., 1983 and 1985). In the EV-treated model, the EV injection engenders an intractable hypothalamic lesion (Brawer et al., 1978, 1980 and 1983), which is correlated with, but not proven to be causally related to, an observed defective hypothalamic regulation of luteinizing hormone releasing hormone (LHRH) (Simard et al., 1987; Carriere et al., 1988). As well, impaired pituitary luteinizing hormone (LH) storage and release (Simard et al., 1987; Carriere et al., 1988) occur. The cascade of hypothalamic and pituitary defects which develop following EV-injection ultimately lead to the establishment of a unique pattern of gonadotropin secretion to which the ovary ultimately responds by developing a polycystic morphology (Grosser et al., 1987; McCarthy et al., 1987; McCarthy and Brawer, 1989). In this model, naltrexone administration or hemi-ovariectomy induce alterations in the PCO-associated LH pattern (Farookhi et al., 1985; Carriere et al., 1989) and result in significant restoration of ovarian histology and function, suggesting that the polycystic ovarian morphology represents the response of a normal ovary to a specific, abnormal hormonal situation.

Chronic exposure to physiological levels of 17-β-estradiol via a silastic implant leads to the development of a hypothalamic lesion and alterations in hypothalamic opiate binding (Wilkinson et al., 1983 and 1985) which resemble those induced by EV injection. As well, a unique pattern of gonadotropin release and polycystic ovaries are established within eight weeks following implant placement (Brawer et al., 1983;

McCarthy and Brawer, 1989). The plasma gonadotropin patterns and the ovarian histology, however, differ considerably from those seen in the EV-induced polycystic ovarian condition (McCarthy and Brawer, 1989). Since removal of the silastic implant containing 17-β-estradiol is followed by restoration of normal ovarian morphology and function (unpublished results), the polycystic response of the ovaries to chronic estradiol exposure also likely represents the response of an essentially normal ovary to a specific, abnormal pattern of hormonal stimulation, as is the case in the EV-treated model.

The focus of this thesis is on the ovary of rats with polycystic ovarian conditions. An analysis of the polycystic ovaries resulting from both estradiol valerate and 17-β-estradiol treatment will be made. Specifically the role of the androgen producing cells, namely thecal cells and secondary interstitial cells, in these conditions will be examined. Of particular interest are the hypertrophied secondary interstitial cells and follicular thecal cells belonging to structures unique to a polycystic ovary, including precystic and cystic follicles.

As an understanding of the phenomenon of cyclicity is critical to assessing and understanding any disease of reproductive infertility, including PCO, a brief discussion of the role of the hypothalamus, the anterior pituitary gland, and of the ovaries in cyclic reproductive function will be presented. Thereafter, the animal models used to study PCO and the experimental proposals of this thesis shall be discussed directly.

The Hypothalamic-Hypophyseal-Ovarian Axis

Role of the Hypothalamus in Female Reproductive Cyclicity

A collection of neurons in the medial basal hypothal mus (in humans) or in the medial preoptic area (in rodents) synthesize a decapeptide known as luteinizing hormone releasing hormone (LHRH), also known as gonadotropin hormone releasing hormone (GnRH) (see Knobil, 1980, for review). This peptide hormone is released by these neurons into the pituitary portal circulation (Dierschke et al., 1970) in a non-continuous, pulsatile matter (see Knobil, 1980, for review). The LHRH is subsequently transported to the anterior pituitary where it induces the synthesis and release of two closely related glycoprotein hormones: luteinizing hormone (LH) and follicle stimulating hormone (FSH) (Matuso et al., 1971). The signals which initiate the circhoral pulsatile discharges of LHRH originate within the central nervous system (Carmel et al., 1976). However, these hypothalamic signals are modified by exposure to estradiol and other steroidal factors synthesized by the ovary (Fink, 1979). Circulating steroid hormones of ovarian origin feed back on the hypothalamus providing both positive and negative influences on the frequency and amplitude of LHRH release during the course of the cycle (Butcher et al., 1974; McEwen, 1979; Ramey et al., 1987).

Role of the Anterior Pituitary in Female Reproductive Cyclicity

The gonadotropes are regulated by complex signals from both the hypothalamus and the ovary. The response of the gonadotropes to the hypothalamic signal, ie.

LHRH, depends upon the nature of the pulse parameters comprising the signal, ie. amplitude and frequency. With respect to the amplitude, as the dose of LHRH released increases, the quantity of LH and FSH released by gonadotropes also increases in a classic dose-response fashion (Knobil, 1980). The system is saturable in that there is a maximal LHRH dose above which no additional LH or FSH secretion will be elicited (Knobil, 1980). The temporal pattern of the hypothalamic LHRH signal can cause suppression of both LH and FSH secretion, stimulate FSH secretion while suppressing LH secretion, or stimulate the release of both gonadotropins (ie. LH and FSH) (see Knobil, 1980 for review). While experimental results suggest that LH secretion is entirely dependent on the endogenous LHRH pattern, there seems to be a second factor acting synergistically with LHRH to regulate FSH secretion (Culler and Negro-Villar, 1987) as there are instances in which FSH secretion is dissociated from that of LH (eg. the follicular phase of the menstrual cycle or the diestrous phase of the estrous cycle). This factor has not yet been identified.

In addition to modulating the hypothalamic LHRH pattern, ovarian steroids modify gonadotropin secretion by exerting both positive and negative feedback effects directly at the level of the gonadotrope. The positive feedback effects of ovarian estradiol include sensitization of the gonadotropes to LHRH, so that lower concentrations of LHRH are needed to elicit a response (Ramey et al., 1987). This positive or "priming" effect contributes to the LH surge which occurs just prior to

ovulation (Butcher et al., 1974). The negative feedback effects of estradiol on the pituitary occurring during the diestrous phase of the estrous cycle (Gallo and Bona-Gallo, 1985) are related to inhibition of gonadotropin secretion (Butcher et al., 1974).

Role of the Ovary in Female Reproductive Cyclicity

The role of the ovary in the reproductive cycle of mammals is twofold, involving: 1) the production of mature eggs, and 2) the elaboration of steroid and peptide hormones which influence sexual behaviour and which contribute to the regulation of both hypothalamic and pituitary function.

The process of follicular development, ovulation and the development of corpora lutea in the mammalian ovary is well known. The ovary contains a pool of resting germ cells, known as oocytes, contained within follicles. These resting oocytes are surrounded by a single layer of granulosa cells, a basement membrane, and stromal cells. Together, these cellular associations constitute a primordial follicle. Of the many follicles contained within the ovary of an adult cycling mammal, only a restricted number ovulate in response to each gonadotropin surge. Those follicles which do not develop to this ovulatory state will undergo a degenerative process known as atresia.

Growth and maturation of follicles is dependent on gonadotropin stimulation (Richards and Midgley, 1976). The dynamics of follicular growth and cellular differentiation, which are critical to the continued development of a follicle, depend upon specific changes in the content of receptors on follicular cells for both LH and

FSH. Furthermore, these changes in receptor content are themselves regulated by specific interactions with estradiol and FSH (Richards and Midgley, 1976). Initiation of follicular growth, ie. the transition from the primordial to the primary stage, occurs spontaneously (Pederson, 1970). Thereafter, however, continued growth and maturation of follicles is dependent on gonadotropins (Richards and Midgley, 1976).

The transition from the primordial to the primary stage involves proliferation of the granulosa cell layer and the organization of the surrounding stromal cells into a thecal layer external to the basement membrane (Peters, 1969). The cytodifferentiation of the stromal cells into thecal cells involves the acquisition of steroid biosynthetic enzymes and LH receptors (Erickson et al., 1985), and the development of a specialized ultrastructure consisting of extensive smooth endoplasmic reticulum, abundant mitochondria with tubular cristae, and numerous lipid droplets which contain the precursor (ie. cholesterol) for androgen biosynthesis (Fawcett et al., 1969; Erickson et al., 1985). The nature of the stimulus initiating the differentiation process is unknown, but is believed to be directed by signals emanating from the developing follicle itself and to be independent of pituitary signals (Erickson et al., 1985). LH stimulation of fully differentiated thecal cells results in cell hypertrophy and androgen production (Rice and Savard, 1966; Ryan and Petro, 1966; and Fortune and Armstrong, 1977). The granulosa cells of primary follicles contain FSH receptors (Midgley, 1973; Nimrod et al., 1974; Zeleznik et al., 1974). FSH stimulation of these cells results in proliferation of the cells forming the membrana granulosa (Eshkol and

Lunenfeld, 1972), increased aromatase activity and, consequently, increased estrogen production (Uilenbroek and Richards, 1979). The estrogen produced by these cells is not synthesized de novo. Rather, granulosa cells convert C-19 androgens of thecal origin to C-18 estrogens by decarboxylation and aromatization of the "A" ring of the steroid molecule.

As folliculogenesis proceeds, the cells of the membrana granulosa continue to proliferate in response to FSH stimulation, additional thecal stem cells proliferate and differentiate (Erickson et al., 1985), and steroid biosynthesis increases. Eventually, the follicular fluid secreted during the growth process coalesces, and a fluid-filled antral space is formed (McKay et al., 1961). The follicle is now called a secondary or antral follicle. At this stage of follicular growth, the perimural granulosa cells of a few follicles will acquire LH receptors as a result of the synergistic actions of FSH and estradiol (Richards et al., 1976). Most follicles, however, do not. Those secondary follicles with abundant LH receptors on both granulosa and thecal cells are the ones which respond to the LH surge by ovulating, undergoing luteinization and forming corpora lutea, while follicles whose granulosa cells have gained few or no LH receptors respond by undergoing atresia (Midgley et al., 1974; Richards and Midgley, 1976).

Follicles may become atretic at any stage of their development (Uilenbroek, Woutersen and van der Schoot, 1980). Initiation of the atretic process may be due to either an inadequate number of gonadotropin receptors, or to the follicle being

out of synchrony with gonadotropin stimulation (Richards and Midgley, 1976). The pattern of atresia is not uniform and depends on the stage of differentiation which the follicle has reached at the time when it begins to degenerate (Byskov, 1979). In general, the process of follicular atresia involves the death of the oocyte and granulosa cells. Interestingly, the cells of the theca interna survive the degenerative processes afflicting the rest of the follicular cells and undergo a marked hypertrophy. These hypertrophied cells then settle in the region of the old follicle and give rise to a population of cells called secondary interstitial cells (Kingsbury, 1939, Dawson and McCabe, 1951; Rennels, 1951; Guraya and Greenwald, 1968; and Deanesly, 1972). Cytologically and biochemically, secondary interstitial cells continue to exhibit properties of their precursor, the thecal cell, in that they maintain the specialized ultrastructural characteristics of active steroidogenic cells (Carithers and Green, 1972; Mori and Matsumoto, 1973; Al-Mehdi, 1979; and Erickson, 1983), they express LH receptors, and they continue to respond to LH by producing androstenedione (Rice and Savard, 1966; McNatty et al., 1979; and Erickson, 1983).

Regardless of the developmental state of ovarian follicular structures or their derivatives, the elaboration of steroid hormones by the follicular cells during follicular growth, by cells of the corpus luteum following an ovulation event (notably estrogen and progesterone), and by gonadotropin-sensitive cells of the interstitium will in turn affect the nature of the hypothalamic and pituitary signal to which they respond by the feedback mechanisms described.

Indeed, the phenomenon of reproductive cyclicity is complex, and depends upon intricate reciprocal interactions between the hypothalamus, the pituitaries and the ovaries. How can this balance which support cyclicity, once established, be disrupted to effect the development of polycystic ovaries?

Experimental Manipulations Leading to PCO

A wide range of experimental manipulations result in persistent vaginal cornification, anovulation and polycystic ovaries bilaterally in laboratory rats. For example, treating neonates with testosterone (Gorski, 1969), adults with dihydroepiandrosterone (DHEA) (Parker and Mahesh, 1976), or hypothyroid rats with human chorionic gonadotropin (hCG) (Copmann and Adams, 1981), all result in a polycystic ovarian condition. As well, conditions of prolonged light exposure (Campbell and Schwartz, 1980; and Daane and Parlow, 1971), luteinizing hormone releasing hormone antibody administration (Popkin et al., 1983), implantation of estradiol benzoate crystals into the anterior hypothalamic area (Kawakami and Visessuvan, 1979), anterior hypothalamic deafferentation (Halasz, 1969), aging (Ascheim, 1976), administration of estradiol valerate (Brawer et al., 1978 and 1986; Mobbs et al., 1984), and subcutaneously implanted estradiol (E_2)-containing chronic release capsules (Brawer et al., 1983) will also result in PCO.

In spite of the hypothalamic and pituitary impairments produced by these different treatments, many of these rats with PCO are still capable of forming corpora lutea in response to certain experimental manipulations. The polycystic ovaries in both the neonatally androgenized and the EV-induced models form corpora lutea in response to an LHRH challenge (Hahn and McGuire, 1978; Hemmings et al., 1983). The induction of corpora lutea is accompanied by the disappearance of cystic follicles from both ovaries, probably by passive compression (Convery et al., 1989).

Hypothalamic and pituitary pathologies, however, persist. Hemi-ovariectomy results in restoration of normal ovarian histology and ovulatory cyclicity within one week in the EV-treated rat (Farookhi et al., 1985; Convery et al., 1989). Again, hypothalamic, pituitary and hormonal abberations persist. In the DHEA-treated, constant light-induced and E_2-implanted models, normal ovarian morphology and ovulatory capacity are restored following the cessation of treatment (Parker and Mahesh, 1976; Daane and Parlow, 1971; and unpublished results, respectively). The fact that cyclic reproductive function can be restored to a polycystic ovary, despite continued dysfunction of the brain and pituitary, further support the notion that the histologically definitive polycystic condition (PCO) does not reflect an intrinsic ovarian pathology.

In our laboratory, two models of the polycystic ovarian condition have been extensively studied and characterized: EV-induced PCO and PCO which results from chronic exposure to physiological levels of 17-β-estradiol. These two models will be used in this thesis. The specific changes in the hypothalamus, pituitary and ovaries in these models are described below.

EV-Induced PCO Model

Hypothalamic and Pituitary Defects Associated with EV-Induced PCO

A single, 2mg injection of a long acting estrogen, estradiol valerate (EV), given to young cycling rats will induce a series of progressive changes along the hypothalamo-hypophyseal-gonadal axis leading to anovulatory acyclicity, persistent vaginal cornification and the development of polycystic ovaries within twenty-eight days (Brawer et al., 1989). In the hypothalamus, multifocal lesions in the arcuate nucleus (Brawer et al., 1978 and 1980), an increased number of naloxone binding sites (Wilkinson et al., 1983), and defective regulation of LHRH secretion (Simard et al., 1987; Carriere et al., 1988) have been observed Pituitary abberations include a decreased pituitary LH content (Schulster et al., 1984), decreased LHRH-stimulated LH secretion (Hemmings et al., 1983), and a depressed number of LHRH receptors on pituitary gonadotropes (Carriere et al., 1988). Basal concentrations of serum LH at eight weeks is low, while that of serum FSH is in the high-normal range (Hemmings et al., 1984; Schulster et al., 1984; Simard et al., 1987), as is the pituitary FSH content (Simard et al., 1987). Thus, all facets of LH production appear to be selectively compromised, while FSH production is intact.

Development of a Histologically Definitive, EV-Induced Polycystic Ovary

The sequence of events leading to the development and expression of polycystic ovaries seems to occur in two phases (Brawer et al., 1986). The first, encompassing the period of time from the day of EV-injection to four weeks thereafter, is

characterized by a steady decrease in the population size of follicular structures of all ranges of diameter, accompanied by a decrease in ovarian weight. Although follicular loss occurs uniformly in follicles of all diameters, a selective enhancement in atresia amongst large secondary follicles is observed during this period in time. By as early as 16 days post EV-injection, an absence of Graafian follicles is observed. By 28 days, corpora lutea are absent, and large, fluid-filled cystic follicles are established bilaterally (Brawer et al., 1978, 1986, 1988 and 1989). Another interesting morphological characteristic of these ovaries is the presence of luteinized granulosa or thecal cells, occurring in clusters circumscribed by a basement membrane or diffusely scattered throughout the stroma. Although these are most likely secondary interstitial cell clusters, they are observed much more frequently in these ovaries versus a normally cycling ovary. Grossly, the ovaries are smaller than their age-matched, untreated cycling counterparts, and can be further distinguished on gross examination by the presence of very prominent, large, fluid-filled protrusions.

The second phase in the development of the polycystic ovarian condition, lasting from day twenty-eight to day fifty-six, is characterized by the achievement of a steady-state population size of all follicles and by non-selective atresia. The degree of atresia in the affected follicles during this phase, however, is substantially more far-reaching.

As the changes leading to the establishment of cystic follicles in the polycystic condition of an estradiol-valerate treated ovary are stabilized by fifty-six days following

hormonal treatment (Brawer et al., 1986 and 1989), eight week ovaries will be used in this study.

Histological Features of an EV-Induced Polycystic Ovary

There are three types of follicular structures which are unique to this EV-induced polycystic ovary. The most characteristic of these, the follicular cyst, consists of a highly attenuated granulosa cell layer, a hypertrophied thecal cell layer, and occasional macrophages lining the antral surface of the membrana granulosa. The second type, the precystic follicle (Brawer et al., 1986 and 1989), resembles the cyst except for the presence of irregular and often rather extensive patches of degenerating granulosa cells along the antral surface of the membrana granulosa. In light microscopic sections of epon-embedded ovaries, the thecal cell layer of these two types of follicles appears to consist primarily of large, polygonal cells filled with lipid ghosts, with a few small fusiform cells scattered in between. The third type of follicular structure found in these polycystic ovaries, identified by Brawer et al. (1989) as a Type III large follicular structure, is characterized by a large antral space circumscribed by multiple layers of healthy granulosa cells. The thecal cell layer consists of a diffuse layer of small, fusiform cells, resembling those characteristic of healthy, developing follicles. The Type III large follicular structure differs from Graafian follicles of normal cycling ovaries in that it is a larger structure, mitotic figures are seen amongst perimural granulosa cells, and they do not contain ova (Brawer et al., 1989; Convery et al., 1989). Paradoxically, the Type III large follicular structure is the only follicular

structure unique to the polycystic ovary in which granulosa cells bind LH (hCG) (Brawer et al., 1989) and is, therefore, the only structure which could be readily luteinized following an LH surge. However, the lack of corpora lutea in these polycystic ovaries suggests that this does not ordinarily happen. The nature, function and role of this follicular structure remains to be elucidated.

Many of the cysts observed in eight week ovaries exhibit patches of degenerating granulosa cells at intervals along an otherwise healthy-looking mural membrana granulosa. This feature is not characteristic of cysts from later time intervals (Hemmings et al., 1983; Schulster et al., 1984; Brawer et al., 1986). The role atresia plays in the two phases of development of polycystic ovaries, and the appearance of these cysts, has raised speculation that true follicular cysts may be products of partial or arrested atresia (Brawer et al., 1986). This possibility is further supported by the observation that the hyperthecosis characteristic of cystic follicles is also characteristic of atretic secondary follicles (Byskov, 1978). Furthermore, the presence of severely atretic secondary follicles at fifty-six days, similar to those observed at earlier time intervals following EV injection but rarely if ever seen in older cystic ovaries, suggests that atresia plays an important role in the ultimate modelling of this polycystic ovary and that cystic follicles may be the consequence of an arrest of the atretic process (Brawer et al., 1986).

Endocrine Features Associated with the EV-Induced Polycystic Ovarian Condition

The histological evolution of polycystic ovaries in this model coincides with the development of a unique low amplitude, high frequency pattern of LH. Although the pattern is pulsatile, the regularity in the frequency and the amplitude of the pulses is markedly different versus those characteristic of pulses of the estrous phase of the rat estrous cycle (Grosser et al., 1987). The FSH pattern is also pulsatile and is closely synchronized with the LH pattern (Grosser et al., 1987). The characteristic patterns emerge between two and four weeks after EV treatment, ie. coincident with the emergence of definitive cysts within the ovaries. Furthermore, they are observed in all animals with established PCO, regardless of the duration of the condition (McCarthy et al., 1988). Based on these findings, Grosser et al. propose that this unique plasma gonadotropin pattern, rather than the mean serum gonadotropin concentration, is causal to the establishment and critical to the maintenance of the polycystic ovarian syndrome in this model.

Radioautographic studies conducted on EV-treated ovaries to assess their sensitivity to LH indicate that cyst formation coincides with the loss of sensitivity of precystic and cystic follicles to LH. Binding of ^{125}I-hCG (an LH analogue used in radioautographic studies because of its stability [Richards and Midgley, 1974]) in precystic follicles is scant and limited to the cells of the theca interna (Brawer et al., 1989; Richard, 1988). Radiolabelled hCG binding in cystic follicles is absent amongst cells of the membrana granulosa and is rare or altogether absent in the theca interna.

In contrast to precystic and cystic follicles, cells of both the perimural membrana granulosa and cells of the theca interna in type III large follicular structures show intense and dense patches of labelling. These structures, then, are presumably LH-sensitive. Labelling of clusters of secondary interstitial cells is highly variable in these polycystic ovaries, varying from dense to absent. The theca interna of normal and atretic follicles bind hCG. The degree to which they bind hCG is similar to binding reported for analogous structures in a non-cystic ovary (Bortolussi et al., 1979; Shaha and Greenwald, 1982). Thus, the precystic and cystic follicles are truly unique, not only structurally but, as well, in their LH binding characteristics. As well, despite the structural homology between cystic theca and the thecal cells of atretic follicles, there must be functional differences between them as they demonstrate marked differences in their capacity to bind hCG (or LH) (Richard, 1988; Brawer et al., 1989).

Chronic Estradiol (E_2) Exposure-Induced PCO Model

Hypothalamic and Pituitary Defects Associated with E_2-Induced Polycystic Ovarian Condition

The extent to which chronic exposure to physiological plasma concentrations of estradiol, delivered by means of chronic release implants, affect the hypothalamo-hypophyseal-ovarian axis of rats to yield a polycystic ovarian condition is less defined than it is for the EV-treated PCO model. Within three weeks following placement of the E_2-containing implants, cyclicity is arrested, and persistent vaginal cornification and anovulation ensue. A definitive polycystic ovarian condition is fully established by at least eight weeks after placement of the silastic implant. This condition persists unless the capsule is subsequently removed (unpublished results). Intact or ovariectomized E_2-implanted animals develop a lesion in the anterior hypothalamus and express enhanced binding of opiates in the anterior hypothalamus within ten weeks following initiation of treatment (Wilkinson et al., 1983 and 1985), as do EV-treated rats with PCO (Brawer et al., 1978). These estradiol-induced effects can be expressed in castrated rats, whereas the development of the hypothalamic pathologies following EV-injection requires the presence of the ovaries (Brawer et al., 1980).

The pituitary defects associated with this model have not yet been identified, although a decrease in pituitary weight is reported by Wilkinson et al. (1985) ten weeks after initiation of chronic estradiol exposure.

Histological Features of an E_2-Induced Polycystic Ovary

The ovaries from E_2-treated animals, in contrast to those from EV-treated animals, are large and smooth surfaced. Non-atretic large secondary follicles are rarely seen in these ovaries. Corpora lutea are altogether absent. The cystic follicles observed in these ovaries are markedly different than those observed in the ovaries of EV-treated animals. They are more numerous, smaller, and are characterized at the light microscopic level by an unusually thick theca interna comprised of hypertrophied, polygonal cells filled with lipid ghosts. The thecal cell layer in these cysts is approximately four to five times the thickness of that in the cysts of EV-treated animals. The granulosa cell layer consists either of a single layer of cells or several layers of degenerating cells. Because of the differences in the size of the cystic structures observed in the ovaries of these two different PCO models, the cysts from an EV-induced polycystic condition may be subsequently referred to as macrocysts and those from a polycystic ovary induced by chronic exposure to 17-β-estradiol as microcysts.

As was observed in the EV-induced polycystic ovaries, numerous clusters of secondary interstitial cells occur scattered throughout the stroma. However, these cell clusters are larger and more frequently observed as compared to an EV-treated ovary. Although the size and shape of some of these clusters suggests that they may be derived from collapsed cysts, the large size and frothy appearance of the cells of some of these cell clusters as observed in epon-embedded light microscopic sections, due to

their engorgement with lipid ghosts, suggests a different origin (McCarthy and Brawer, 1989; and personal observations).

Endocrine Features Associated with the E_2-Induced Polycystic Ovarian Condition

Unlike the EV-treated rat with PCO, the E_2-implanted rat exhibits a complex plasma LH pattern. McCarthy et al. (1989) demonstrated two types of episodic LH secretion in these animals. The first consists of short, frequent, sharply delineated low amplitude pulses. This pattern is very similar to that seen consistently in rats with EV-induced PCO (Grosser et al., 1987). These short, low amplitude pulses are interrupted at regular intervals by the second type of pulse, consisting of episodes of LH release of high amplitude and long duration. Although FSH patterns generally conform with the LH patterns, definitive FSH peaks are not observed to correlate with those of LH (McCarthy et al., 1989). This is in contrast with the synchronous gonadotropin patterns reported for the EV-induced model of PCO (Grosser et al., 1989) and is suggestive of a second mechanism involved in FSH regulation in these E_2-implanted animals.

Significance of Using Two Models To Study Polycystic Ovarian Conditions

The characteristics of the EV-induced and E_2-implanted models of polycystic ovarian condition are similar to two expressions of cystic ovarian disease in humans. The morphology of the EV-induced polycystic ovary resembles what is called a multifollicular ovary, seen in women with hypothalamic amenorrhea associated with weight loss (Adams et al., 1985). The ovaries of women with this pathology contain several very large cystic follicles, and do not exhibit stromal hypertrophy. In contrast, the human polycystic ovary in the classical Stein-Leventhal syndrome is enlarged, contains multiple small cysts and an extensively hypertrophied stroma (Adams et al., 1986). This is similar to the ovarian morphology in rats receiving subcutaneous implants containing estradiol (Brawer et al., 1983; McCarthy and Brawer, 1989).

In addition to the similarities in ovarian morphology, serum LH patterns in human and rat cystic ovarian conditions show similarities. In hypothalamic amenorrhea, the LH pattern is greatly suppressed, exhibiting only occasional low amplitude pulses. Some patients also experience larger pulses at night (Khoury et al., 1987). The corresponding polycystic condition in the EV-treated rat is associated with a highly suppressed pattern of LH release, consisting of low amplitude, high frequency pulses. In marked contrast to the pattern of gonadotropin release in patients with hypothalamic amenorrhea, women with Stein-Leventhal syndrome express an exaggerated pattern of LH release, consisting of high amplitude pulses arising from a higher mean nadir (Rebar et al, 1976; Waldstreicher et al., 1988). Although the

frequency and nadir of the highly irregular pattern of LH secretion observed in animals with a polycystic condition induced by chronic E_2 exposure does not correspond to the pattern in the human, the large LH surges observed are considered to reflect a highly stimulatory pattern of secretion (McCarthy and Brawer, 1989), one which may or may not be comparable to that of the Stein-Leventhal syndrome.

In addition to the parallels between ovarian morphology and plasma gonadotropin patterns in humans with hypothalamic amenorrhea and rats with an EV-induced polycystic ovarian condition, both disorders can be ameliorated by blockading the opiatergic system which is involved in regulation of LHRH neurons in the hypothalamus (Khoury et al., 1987; Wildt and Leyendecker, 1987; Carriere et al., 1989).

THESIS PROPOSAL

Rationale

Although there is good reason to implicate the alterations in hypothalamic LHRH or pituitary gonadotropin secretion as the underlying cause for the generation of ovarian cysts, the role played by the ovary in maintaining the established polycystic condition cannot be considered insignificant. In the case of human PCO, ovarian wedge resections have been used successfully to temporarily alleviate the acyclic condition of these patients (Goldzieher, 1981). In rats with an EV-induced polycystic ovarian condition, ovulatory function resumes following hemiovariectomy, despite continued dysfunction at the hypothalamic and pituitary levels of the axis (Farookhi et al., 1985; Convery et al., 1989). Removal of the E_2-containing silastic implants after the polycystic morphology has been established will also be followed by a restoration of morphology and function to the previously acyclic, anovulatory ovaries (unpublished results). The fact that expressions of PCO are reversible strongly suggests that: changes in ovarian function in PCO are not the cause of the disruption in cyclic reproductive function; and polycystic ovaries are not an expression of ovarian pathology. PCO may be simply a potential developmental condition of a normally functioning ovary which is a manifestation of a primary pathology either at the level of the hypothalamus or pituitary. If this is in fact the case, what is a polycystic ovary?

The existence of specialized populations of ovarian interstitial cells is physiologically significant because the androgens they secrete are of major importance.

Androgens are obligatory precursors for estrogen biosynthesis (Baggett et al., 1956; Ryan and Smith, 1961; Engel, 1973), estrogens being essential for normal reproductive function. In addition, androgens induce follicular atresia (Payne et al., 1956 and 1958; Louvet et al., 1975). In polycystic ovarian disease, the ovaries are anovulatory and acyclic. Furthermore, follicular atresia seems to play an important role in the modelling of a polycystic ovary (Brawer et al., 1986 and 1989). What role do the interstitial cells play in the development and maintenance of PCO?

Interstitial cell populations are located in both the theca interna of follicles and the interstitial compartment of the ovary. All interstitial cells arise from a population of unspecialized mesenchymal cells in the stromal compartment. During the differentiation process, the interstitial cells develop a specialized ultrastructure suited to steroid biosynthesis (Fawcett et al., 1969) and acquire LH receptors (Midgley, 1973; Richards and Midgley, 1976) which are functionally coupled to androgen biosynthesis (Erickson and Ryan, 1976; Richards and Midgley, 1976, Fortune and Armstrong, 1978). Despite the sensitivity of these cells with LH receptors to pituitary stimulation, cytodifferentiation is believed to commence independently of the pituitary (Eshkol and Luhenfeld, 1972). A developing interstitial cell has a range of functional options. A thecal cell in a developing follicle may undergo further differentiation to become an atretic follicular thecal cell and subsequently a secondary interstitial cell (reviewed in Erickson, 1985). If a follicle develops to the point of ovulation, it will undergo luteinization and become a thecal lutein cell of a corpus luteum. In a polycystic ovary,

a thecal cell from a developing follicle can become an atretic follicular thecal cell. This cell may then become a secondary interstitial cell, or may possibly follow a different pathway toward becoming a cystic thecal cell. As studies on the follicular dynamics of developing macrocystic ovaries (Brawer et al., 1986 and 1989) and recovering macrocystic ovaries (Convery et al., 1989) suggest that a macrocyst is an inert structure which seems to be the result of an arrest of the atretic process, it is also possible that a cystic thecal cell is a direct derivative of a healthy follicular thecal cell, rather than of an atretic thecal cell. In the microcystic ovary, interstitial cells may follow pathways similar to those described above. In light microscopic sections of these ovaries, McCarthy and Brawer (1989) observed secondary interstitial cell clusters approximating the shape and size of a microcystic follicle, and suggested that some of the secondary interstitial cell clusters within these ovaries may derive from collapsed cysts.

In consideration of the above, we have asked what the morphology of these interstitial cell populations means. How are cysts related to other follicular structures? Do all secondary interstitial cell clusters have the same origin? Do differences in morphology reflect differences in functional capacity between thecal cells and thecal derivatives? If differences in functional capacity are found between these cells in a macrocystic or microcystic ovary, can the different functional types of thecal cells and thecal derivatives be related to the characteristics of the disorder (eg. gonadotropin levels and steroid levels)?

Proposal

In order to assess differences in the structural and functional characteristics among thecal cells and thecal derivatives within EV-induced and E_2-induced polycystic ovaries, five indices of cytodifferentiation and steroid synthetic activity will be examined. The interstitial cells under study include healthy secondary, atretic secondary, precystic and cystic follicular thecal cells, and secondary interstitial cells. The indices to be examined include: alkaline phosphatase expression, LH binding capacity, mitochondrial area, lipid droplet area, and cell size.

The expression of alkaline phosphatase has been implicated to reflect gonadotropin stimulation and steroidogenic activity in thecal cells and thecal derivatives in the ovary (McKay et al., 1961; Pinkerton et al., 1961; Kent, 1974; Ross, 1974, Kent and Ryle, 1975). Alkaline phosphatase expression by the cells listed above will be evaluated at the light microscopic level in macrocystic (EV-treated) and microcystic (E_2-implanted) ovaries using an immunohistochemical marker for alkaline phosphatase. Activity within the different cells should reflect differences in tropic hormone stimulation and steroidogenic activity.

The capability of a cell to bind LH is another index of its sensitivity to tropic hormone stimulation and steroidogenic capacity (Dimino, 1977; Dimino and Berman, 1979; Midgley, 1973; Richards et al., 1976; Rowe et al., 1981 and 1986). LH binding sites can be localized using electron microscopic radioautography on ovarian tissue exposed in vivo to either ^{125}I or ^{131}I-hCG or LH. Both hormones share immunologic

(Franchmont, 1970), chemical (Closset and Hennen, 1973; Bahl, 1972; Morgan and Canfield, 1971) and biological properties (Lunenfield and Eshkol, 1967). Both LH and hCG bind with high affinity and specificity to the same receptor (Lee and Ryan, 1972b; Kammerman et al., 1972a,b; Rajaniemi and Vanha-Perttula, 1972; Leindenberger and Reichert, 1971; Koch et al., 1974; Kammerman and Canfield, 1972). As well, both hormones can be iodinated using the chloramine T method and retain their biological activity (Midgley, 1966; Lunenfield and Eshkol, 1967; Lee and Ryan, 1972; and Dufau, 1972). As hCG is less damaged by iodination and is more stable (Ryan and Lee, 1976), it was chosen as the ligand for this study. Thecal and secondary interstitial cell LH/hCG binding sites will be evaluated in the cell types listed within macrocystic and microcystic ovaries using electron microscopic radioautography.

The expression of surface LH receptors enables thecal precursors to differentiate from fibroblast-like precursors to polygonal cells with the ultrastructural characteristics of steroid secreting cells (reviewed in Erickson, 1985). The ultrastructural characteristics of such a cell include the presence of smooth endoplasmic reticulum, mitochondria and cholesterol-containing lipid droplets (Davies and Broodus, 1968; Fawcett et al., 1969). LH stimulation of differentiated thecal cells and thecal derivatives results in an increase in mitochondrial size (Rowe et al., 1981), reorganization of mitochondrial cristae from lamellar to tubulovesicular (Dimino et al., 1979; Rowe et al., 1981), and an increase in the ability of mitochondria to synthesize

pregnenolone and progesterone (Dimino, 1977; Dimino and Berman, 1979; Rowe et al., 1981; Rowe et al., 1986). Hypophysectomy results in a reduction in size, number of mitochondria, and number of cristae in mitochondria. As well, the amount of lipid contained within interstitial cells increases appreciably (Carithers and Green, 1972 a,b). Because lipid droplets and mitochondria are involved in steroid biosynthesis and because the size of both is affected by LH, lipid droplet area and mitochondrial area will be measured by morphometric analysis on electron microscopic radioautographs of thecal and secondary interstitial cells from macrocystic and microcystic ovaries. These two parameters will provide an additional index of tropic hormone stimulation and steroidogenic capacity within different classes of thecal cells in these ovaries.

Thecal cells and secondary interstitial cells are often classified as "normal" or "hypertrophied". Hypertrophied cells are considered to be highly steroidogenic (Carithers and Green, 1972a,b; Erickson, 1985). An index of thecal cell size will be determined by measuring perpendicular diameters of cells at the light microscopic level. This parameter will provide an additional index in the consideration of the steroidogenic activity of thecal and secondary interstitial cells.

MATERIALS AND METHODS

Animal Housing and Selection

The animals used in these experiments, Female Wistar rats (6 weeks of age, 175-200g body weight) were purchased from Charles River Ltd., St. Constant, Quebec. They were maintained under conditions of controlled light (14 hours light/ 10 hours darkness) and temperature (22°C) and were allowed free access to pelleted rat food and water. Following a two week acclimation period, vaginal smears were monitored daily to establish the occurrence of normal estrous cycles (Schwartz et al., 1964). Animals displaying at least two consecutive four day estrous cycles were selected for this study.

Estradiol Valerate-Treated Animals

Thirty animals were lightly anaesthetized with ether and given a single 2 mg intramuscular injection of estradiol valerate (EV) dissolved in .2 ml sesame oil (Squibb Canada, Inc., Montreal, Quebec) in order to induce PCO (Brawer et al., 1978). Since it has been well established that an injection of sesame oil alone does not alter either the morphology or function of the hypothalamo-hypophyseal-gonadal axis (Brawer et al., 1978 and 1986; Farookhi et al., 1985; Hemmings et al., 1983, Schulster et al., 1984; Simard et al., 1987), sesame oil-injected animals were not prepared as controls for this study. Although cystic follicles are present within the ovary twenty- eight days following injection of estradiol valerate (Brawer et al., 1986 and 1989), a period of fifty-six days was allowed to elapse after injection as cysts are fully expressed by this

time and the morphology of the ovary from this time point on remains constant (Brawer et al., 1986; Schulster et al., 1984). Eight weeks after EV-treatment, those animals which demonstrated unequivocal and sustained cornified vaginal smears during the two prior weeks were chosen for further study.

Animals Receiving Estradiol-Containing Implants

An additional twenty animals were lightly anaesthetized with ether and Polydimethylsiloxane (Silastic) capsules containing 17-β-estradiol were implanted subcutaneously. The silastic capsules were prepared according to the method of Stratton et al. (1973) using a 2 mm long piece of polydimethylsiloxane tubing with an outer diameter of 3.18 mm and an inner diameter of 1.98 mm (no. 602-305, Dow Corning, Midland, MI). The release rate of these capsules was approximately 2.4μg/cm day (Robaire et al., 1979 and 1982). They have been shown to maintain a constant plasma estradiol concentration of approximately 50 pg/ml (Brawer et al., 1983). Six weeks after placement of the implants, vaginal smears were monitored daily. All animals used in this study were in a state of sustained vaginal cornification between the sixth and eighth week after implant placement. This interval was selected as the polycystic morphology of the ovary is fully expressed by eight weeks after placement of the implant (Dr. J.R. Brawer, unpublished observation).

Experimental Procedure - Alkaline Phosphatase Study

Eight weeks after either EV treatment or silastic capsule implantation, two groups of eight animals, each demonstrating persistent vaginal cornification during the

prior eight days, were selected for this study. As well, eight untreated, cycling, age-matched controls maintained under identical housing conditions as the hormonally treated animals were used. The animals were sacrificed by decapitation and their ovaries were removed, decapsulated, weighed, and snap frozen in liquid isopentane (Sigma, St. Louis, MO) at -40°C. The ovaries were then stored in a biofreezer (-90°C) until sectioned.

Frozen whole ovaries were mounted on a chuck using O.C.T. compound (Tissue-Tek, Miles Scientific) and sectioned at 20μm intervals on a Reichert cryotome maintained at -20°C. The sections were thaw-mounted on gelatin-coated glass slides and then stored at -90°C until immunostained for alkaline phosphatase activity.

Prior to staining, the sections were removed from the biofreezer and air dried for twenty minutes at room temperature. They were then washed in cold phosphate buffered saline (PBS) and subsequently fixed in absolute ethanol at 4°C for thirty seconds (Ponder and Wilkinson, 1981). For the immunohistochemical demonstration of alkaline phosphatase activity, the standard ABC Vectastain method using antibodies against alkaline phosphatase H (Vector laboratories, Burlingame, California) was employed. Tissue sections were incubated in a humidified chamber in a solution containing rabbit anti-alkaline phosphatase H antibodies, biotinylated goat anti-rabbit immunoglobulin molecules, and an avidin-biotin complex coupled with phosphatases. The optimal incubation time was determined by incubating sections for varying amounts of time between fifteen and thirty minutes. The best incubation time was

found to be twenty-three minutes, as incubation times longer than this resulted only in an increased intensity of the reaction with no variation in localization of the reaction.

Following a twenty-three minute incubation period in the ABC-AP substrate solutions, the sections were washed for five minutes in several changes of glass-distilled water, counterstained with toluidine blue, air dried and coverslipped.

Control sections were obtained by incubating ovarian tissue sections in the substrate solution prepared without the primary antibody. Background staining, when observed, was very low.

Alkaline phosphatase expression was assessed in all classes of follicles (ie. primary, secondary, Graafian, precystic and cystic), in corpora lutea and in the cells of the stromal compartment. Immunoreactivity for alkaline phosphatase was evaluated by visual inspection at the light microscopic level. A rating scale will be used in the text and in a summary chart. The units which will be used to index alkaline phosphatase expression include: "O", "$\pm$", "(+)", "+" and "++". "0" denotes no activity, "$\pm$" an occasional positive reaction, "(+)" a weak reaction; "+" a consistent and definitive positive reaction, and "++" a strong reaction. Because vascular endothelial cells of the rat ovary show considerable alkaline phosphatase activity and may, therefore, cause occasional diffusion artifacts leading to the staining of structures which may not be specialized with regard to alkaline phosphatase activity, an asterisk is used to signify when at least part of the reaction observed for a particular structure

is given by blood vessels.

Experimental Procedure - hCG Study

Preparation and Administration of hCG Radioligand

Eight weeks after EV-treatment and capsule implantation, two groups of nine animals each were anaesthetized by an intraperitoneal injection of 15% urethane (Ethyl Carbonate) at a dose of 1ml/100g body weight. Subsequently, each animal received an intrajugular injection containing approximately 100 x 10^6 cpm of ^{125}I-hCG diluted in 0.2 ml of PBS. The quantity of radioactivity used was based on previous studies in our laboratory which indicated that this dosage results in a level of radioactivity within the ovary which is 100-700x in excess of background levels and, consequently, is sufficient to provide a good representation of the number and location of LH binding sites present within the ovary (M. Richard, 1988 and Brawer et al., 1989).

The iodination of hCG was performed using the Chloramine T method as described by Ireland and Richards (1978). Highly purified human chorionic gonadotropin (hCG) (CR-121, 13,450 IU/mg) (Morgan et al., 1974) used as the iodinated ligand was a gift from the Center for Population Research of the NICHDD of the National Health Institute (NIH). The specific activity of the ^{125}I-hCG prepared for this study was approximately 50 μCi/μg for the EV-treated animals and approximately 45 μCi/μg for those animals chronically exposed to estradiol via. a silastic implant.

As a control for the specificity of the radiolabelled ligand, three EV-injected animals and three E_2-implanted animals were injected with the same dose of ^{125}I-hCG along with a thousand fold excess of unlabelled hCG (Ayerst Laboratory, Montreal, Quebec). Labelling observed in the ovaries of these animals after radioautographic processing would represent non-specific labelling.

A period of thirty minutes was allowed to elapse after injection of the radiolabelled ligand before sacrificing the animals. This exposure time was selected based on findings of Rajeniemi et al. (1974) and Han et al. (1974) which indicates that there is no difference in the level of labelling in the ovary at five or sixty minutes post ^{125}I-hCG administration.

Animals were sacrificed by perfusion via. the abdominal aorta, according to the procedure described by Vitale et al. (1973). The abdominal cavity was exposed through a midline abdominal incision and the intestines were retracted in order to expose both the ascending vena cava and the abdominal aorta. After the two vessels were separated, the descending aorta was clamped immediately above the iliac bifurcation. An 18 gauge needle was introduced into the aorta, above the clamp, and perfusion with lactated Ringer's solution was begun. Upon clearance of blood from the kidneys, a second clamp was placed just above the renal vein, an incision was made in the right renal vein, and the perfusate solution was switched to a 0.12M phosphate buffered 1% formaldehyde - 1% gluteraldehyde solution of pH 7.4 (Karnovsky, 1965). Approximately 150 ml of fixative was perfused through the system.

Following perfusion, the ovaries were removed, decapsulated, weighed, placed in a gamma counter to determine the quantity of radioactivity taken up, and finally placed in fixative overnight.

Preparation of Tissues for Radioautography

The next morning, the ovaries were cut into two pieces each and then washed for five minutes in a cold solution containing dextrose, 0.4% standard phosphate buffer, and calcium chloride. They were then post-fixed in a solution of 2% osmium tetroxide and 2% potassium ferrocyanide for two hours (Karnovsky, 1971). Following post-fixation, the ovaries were washed twice in a 2.4% calcium chloride solution, dehydrated in a graded methanol series, and embedded in epon.

Pale gold sections of 50-100nm were cut from epon blocks using a diamond knife and a Reichert microtome. The sections were mounted on Athen-type EM copper grids (300 mesh) using an aspirator with attached filter paper. Within seven days following the injection of the radiolabelled hCG and perfusion of the animals, the ovarian tissue sections were processed for EM radioautography.

Electron Microscopic Radioautography

The section-bearing grids were coated with Ilford L4 Emulsion (Ilford Photo Canada, Markham, Ontario), exposed for 6 months (exposure time was based on the results of sections from the same ovaries which were processed for light microscopic radioautography) and then developed for fine grain electron microscopic radioautography by the method of Kopriwa (1975). The sections on the grids were

then stained with a solution of 4% uranyl acetate in methanol for 5 minutes, rinsed with glass-distilled water, and counterstained with 0.1% lead citrate for two minutes.

Electron Microscopy

Electron microscopic examination of the ovaries was carried out on either a Siemens 101 or a Phillips 400T electron microscope. Thecal cells were localized to healthy follicles, atretic follicles, precystic and cystic follicles. As well, secondary interstitial cells were localized. Ten thecal cells each from healthy secondary follicles, atretic secondary follicles, precystic follicles (EV-treated ovaries only), cystic follicles and ten secondary interstitial cells from both EV-treated and E_2-treated ovaries were photographed without bias at a magnification of 5,000x. Thus, forty thecal cells from macrocystic ovaries, thirty thecal cells from microcystic ovaries, and ten secondary interstitial cells from macrocystic and microcystic ovaries, were analyzed. For each cell type examined, at least one photograph was taken from each of the six EV-treated animals and each of the E2-implanted animals. In other words, two photographs were taken from the structures within the ovaries of four different animals with either a macrocystic or a microcystic condition, and one photograph was taken from the structures within the ovaries of two different animals with either a macrocystic or a microcystic ovarian condition.

Electron micrographs of thecal and secondary interstitial cells were examined for changes in the size of lipid droplets and mitochondrial area within the cytosol of the various classes of cells. Lipid droplet area and mitochondrial area were measured

with a MicroPlan II image analyzer. Radioautographic grains in each cell were counted from the electron micrographs, according to the guidelines established by Kopriwa and Nadler (1984) for fine grain, solution physical development of electron microscopic radioautographs with ^{125}I as the isotope. Because of the size variations between thecal and secondary interstitial cells of the same origin and between the different classes of cells, grain counts were expressed as per 1,000μm cell surface length as the receptor is located on the plasma membrane (Rajaniemi and Vanha Perttula, 1972; Rajaniemi et al., 1974). The surface length of the cell surface was measured by tracing the plasma membrane using a MicroPlan II image analyzer.

Determination of Cell Size

The cell size for each type of thecal cell and for secondary interstitial cells was measured using a light microscope with an ocular micrometer. Measurements were made at a magnification of 2,000X. Perpendicular diameters of four cells each from healthy secondary follicles, atretic secondary follicles, precystic follicles, cystic follicles and secondary interstitial cells from five different ovaries were taken. Measurements were made on cells which were cut through the plane where the nucleolus of the cell was visible. The average of these two measurements was then calculated to provide an index of cell areas for thecal cells from healthy follicles, atretic follicles, precystic and cystic follicles, and secondary interstitial cells.

Analysis of Data

Mean cell size of thecal cells from healthy follicles, atretic follicles, precystic follicles (macrocystic condition only), cystic follicles and secondary interstitial cells from both macrocystic and microcystic ovaries were compared using Student's t-test. Differences were considered significant at $p<0.05$.

The mean lipid droplet area for each cell type examined (ie. healthy secondary follicular theca, atretic secondary follicular theca, precystic theca [macrocystic condition only], cystic theca, and secondary interstitial cells) was calculated by dividing the total lipid droplet area from the ten cells in that category by the total number of lipid droplets scored in those ten cells. Mean lipid droplet area histograms were generated for both macrocystic and microcystic ovaries. In addition, the percentage of the cytoplasmic area of the cell profile occupied by lipid was determined. The cytoplasmic area of the cell profile was calculated by subtracting the nuclear area from the total cell profile area. Nuclear and cell profile areas were measured using a MicroPlan II image analyzer. Multi-group comparisons of the data from each type of ovary were analyzed by one way analysis of variance. A comparison of means between the different classes of thecal or secondary interstitial groups from macrocystic or microcystic ovaries was made using a Student's t-test. Differences were considered significant at $p<0.05$.

Mean area of mitochondrial profiles for each cell type examined was calculated by dividing the total mitochondrial area for the ten cells in that category by the

number of mitochondrial profiles scored in those ten cells. Histograms of mean mitochondrial area were generated for both macrocystic and microcystic ovaries. The percentage of the cytoplasmic area of the cell profile occupied by mitochondrial profiles was again determined. Multi-group comparisons of the data from each type of ovary were analyzed by one way analysis of variance. A comparison of means between the different classes of thecal or secondary interstitial cell groups from macrocystic or microcystic ovaries was made using a Student's t-test. Differences were considered significant at $p<0.05$.

RESULTS

Histological Features of Polycystic Ovaries

Light Microscopic Description of Macrocystic Ovaries

In the estradiol valerate-induced polycystic ovary, primordial and primary follicular populations appear as they do in healthy, control ovaries. The number of secondary follicles contained within the macrocystic ovaries is, however, diminished. Most of the secondary follicles are atretic, and they are unusually small in size. Graafian follicles and corpora lutea are absent from these ovaries.

EV-induced polycystic ovaries contain three histologically distinct large follicular structures which are not observed in untreated, normally cycling ovaries. The first, the macrocyst, is a large structure characterized by an attenuated membrana granulosa (one, or occasionally up to three cell layers thick) and a hypertrophied thecal cell layer (Figure 1). Intermingled with the fusiform granulosa cells, or free in the antral space, are large macrophage-like cells containing dense inclusion granules and frothy, ghost-like droplets. The basement membrane surrounding the membrana granulosa is thicker than in healthy developing follicles or Graafian follicles of a cycling ovary. The hypertrophied thecal cell layer consists of large, polygonal cells which are densely packed with lipid droplet ghosts, giving them the appearance of being luteinized. Their appearance is distinct from thecal cells of healthy follicles, which are small, fusiform in shape, and contain much less lipid. However, they are strikingly similar

in appearance to secondary interstitial cell clusters found scattered throughout the stroma.

The second type of large follicular structure is characterized by a large antrum lined by several irregular layers of granulosa cells in different stages of degeneration (Figure 1). The granulosa cells are polygonal in shape. Phagocytic cells are only occasionally seen interspersed between them. The thecal cell layer is hypertrophied, as is that of a cystic follicle. However, small fusiform cells are intermingled with the lipid-filled, hypertrophied polygonal cells. This structure is referred to as a precystic follicle (Brawer et al., 1986, 1989; Richard, 1989).

The third type of large follicular structure unique to an EV-induced polycystic ovary is the Type III Large Follicular Structure (Figure 2). This structure is larger than preovulatory follicles. It consists of a thick membrana granulosa, an undulated basement membrane, and a diffuse layer of small, fusiform thecal cells with occasional, scattered large polygonal cells. The granulosa cells of this follicle differ from those of a healthy secondary follicle in that they are smaller, more variable in shape, and more densely packed. In addition, mitotic figures are observed in the perimural region of the membrana granulosa. The thecal layer of a Type III Large Follicular Structure differs from that of a healthy developing follicle in that it has a festooned appearance. Grossly, this structure differs from preovulatory follicles in that it is larger and contains no ovum.

Secondary interstitial cell clusters are a normal component of the ovarian stroma, generally thought to be derived from collapsed atretic follicles (Kingsbury, 1939; Dawson and McCabe, 1951; Greenwald, 1968; and Deanesly, 1972). They are unusually abundant in these polycystic ovaries. These polygonal cells are large and are filled with lipid ghosts (Figure 3).

Five classes of interstitial cells from these macrocystic ovaries will be studied: healthy and atretic secondary follicular thecal cells, precystic and cystic thecal cells, and secondary interstitial cells.

Light Microscopic Description of Microcystic Ovaries

The histological differences between ovaries continuously exposed to physiological levels of estradiol for eight weeks and normal, control ovaries are striking. However, like EV-treated ovaries, E_2-exposed ovaries do not contain corpora lutea. As well, large secondary follicles are rarely observed, and those that are, are normally atretic.

In the cortical region of the ovary, numerous small cystic follicles are present (Figure 4). These cystic follicles are considerably smaller than their counterparts in a microcystic ovary (average diameter 740μm versus 229μm, respectively [n=10]). The membrana granulosa of these cystic follicles consists of between one and four layers of degenerating cells and an unusually thick layer of hypertrophied thecal cells. The thecal cell layer is approximately four times the thickness of that of the macrocyst. At the light microscopic level, the cytoplasm of these thecal cells appears to be

entirely occupied by lipid droplets.

The interfollicular (stromal) area of the microcystic ovary is very distinct in its appearance (Figure 4). Numerous extensive clusters of secondary interstitial cells are scattered throughout the stromal area. The cells within these clusters are large, pale staining and frothy. The frothy appearance of these cells reflects the fact that they are engorged with lipid ghosts. The size and shape of some of these cell clusters approximates that of a cystic follicle, suggesting that they may derive from collapsed cysts.

Four classes of cells from these microcystic ovaries were studied: healthy and atretic secondary follicular theca, cystic thecal cells, and secondary interstitial cells.

ALKALINE PHOSPHATASE

A summary of the distribution of the immunohistochemical marker for alkaline phosphatase within the various cells types of ovaries treated with either a single injection of estradiol valerate or exposed to chronic physiological levels of 17-β-estradiol via a silastic implant, along with the distribution in untreated control ovaries, is presented in Table 1.

Alkaline Phosphatase: Primordial and Primary Follicles

In all three types of ovaries studied, no alkaline phosphatase immunoactivity (0) was observed in the membrana granulosa of follicles at any stage of development, whether healthy or atretic.

Alkaline phosphatase expression in the stromal cells encircling the primordial follicle, which have not yet differentiated into thecal cells, is very weak (±) and infrequently observed. In marked contrast, a positive (+) alkaline phosphatase reaction is observed consistently in the cytoplasm of the developing cells of the theca interna of primary follicles (Figure 5).

Alkaline Phosphatase: Secondary and Graafian Follicles

A strong, positive reaction (++) for alkaline phosphatase is observed in cells of the theca interna of healthy secondary follicles within the ovaries of control, EV-treated and E_2-implanted animals. Graafian follicles, present only in control ovaries, also demonstrate a strong positive reaction. Alkaline phosphatase expression is maximal at this stage of follicular development, as the reaction product observed here following immunostaining is the strongest one observed for any cells in the ovary (Figure 6). Staining is observed diffusely within the cytoplasm of these cells, with some cells showing a well defined peripheral cytoplasmic zone which is richer in alkaline phosphatase content. As well, the amount of alkaline phosphatase activity in these cells increases as one moves outward from the basement membrane.

In addition to the staining localized to the cells of the theca interna of these follicles, endothelial cells of thecal capillaries also show a strong, positive reaction (++) following immunostaining (Figure 7).

Alkaline Phosphatase: Atretic Follicles

The theca interna of atretic antral follicles displays a strong, positive reaction (++) for alkaline phosphatase, regardless of the degree of atresia expressed and of the type of ovary from which the section was taken (Figure 8). The density of the reaction product is comparable to that observed in a non-atretic counterpart.

Alkaline Phosphatase: Corpora Lutea

Corpora lutea are observed only in the control ovaries (Figures 6 and 8). Because the sections are prepared from frozen ovaries, resolution of morphological details of the cells is inadequate to permit classification of thecal and granulosa lutein cells. Staining of cells within these structures is highly variable. The cells of corpora lutea which accumulate reaction product following incubation with the enzyme marker are deeply stained (++). In some cases, almost all of the cells comprising the corpus luteum are stained. In other cases, staining is restricted to cells near the central coagulum or to radial strands of cells.

Alkaline Phosphatase: Secondary Interstitial Cells

The immunostaining of secondary interstitial cells is highly variable between the control, EV-treated and E_2-implanted ovary. In control ovaries, immunostaining occurs primarily over vascular endothelial cells. Small clusters consisting of ten or fewer interstitial cells show a moderate (+) reaction to the alkaline phosphatase antibody complex, but these are infrequently observed in the interfollicular spaces and seldom found in the hilar region of the ovary (Figure 9).

In the estradiol-valerate treated ovary, a strong positive reaction for alkaline phosphatase is most prominent amongst vascular endothelial cells. Faint staining occurs over intermittent clusters of twenty or so interstitial cells (±) located both peripherally in the interfollicular spaces and in the region of the hilus. The occurrence of these alkaline phosphatase positive cell clusters is much more frequent than in control (healthy) ovaries, but the staining is substantially weaker.

In cystic ovaries induced by chronic exposure to 17-β-estradiol via silastic implants, small strands of secondary interstitial cells showing a strong positive reaction (++) for alkaline phosphatase are observed in the peripheral and juxta-hilar regions of the ovary. The intensity of the staining of these cells is similar to that observed within the vascular endothelial cells. Occasional highly reactive (++) small, round clusters of cells are observed in the peripheral regions of the cortex (Figure 10). In addition to these highly reactive strands and clusters of cells, smaller clusters of interstitial cells, similar in size to those within an EV-treated ovary and faintly stained by reaction product (±) are observed dispersed throughout the interfollicular areas of the cortex.

Alkaline Phosphatase: Precystic Follicles

Precystic follicles are encountered only within estradiol-valerate treated cystic ovaries. They are distinguished from true cystic follicles by the presence of irregular and often rather extensive patches of degenerating granulosa cells along the antral surface of the membrana granulosa. A moderate staining reaction (+), similar to that

observed over the thecal wreath of primary follicles, but weaker than that observed over thecal cells of antral follicles, is observed over these thecal cells. The vascular endothelial cells are a bit more prominent here as they stain more intensely than the background staining of the cells of the theca interna. The membrana granulosa of these follicles remains negatively stained (0) (Figure 11).

Alkaline Phosphatase: Cystic Follicles

Cystic follicles are observed in both EV-treated and E_2-implanted ovaries, but are absent from control ovaries. In both types of ovaries, the attenuated granulosa cell layer is stained only with toluidine blue (0). The hypertrophied thecal layer characteristic of these cystic follicles is very weakly stained ($\pm$) in comparison to the staining observed on either primary or antral follicles, healthy or atretic in both the macrocystic (Figure 7) and microcystic (Figure 12) conditions. As well in most of the cystic follicles, only the two layers of thecal cells adjacent to the basement membrane are stained by the enzyme marker. In no instance is the thecal ring totally unreactive. The endothelial cells within this layer of cells remain strongly reactive (++). Consequently, it is possible that some of the staining is due to diffusion of the reactive product from the vascular system.

ELECTRON MICROSCOPIC CYTOLOGY OF THECAL AND SECONDARY INTERSTITIAL CELLS

Estradiol Valerate Treated Animals - Macrocystic Ovarian Condition

Light Microscopic Analysis of Cell Size

A mean index of cell size of thecal cells from healthy and atretic secondary follicles, precystic and cystic follicles, and of secondary interstitial cells, is summarized in Figure 13.

The mean cell size of healthy secondary follicular thecal cells $\pm$ standard error of the mean (S.E.M.) is $9.8 \pm .4\mu$. Their size is significantly smaller than the mean cell size of the other four cell types examined ($p < .001$). Mean atretic secondary follicular thecal cell size is $12.0 \pm .3\mu$. Mean cell size of precystic and cystic thecal cells is $11.2 \pm .3\mu$ and $11.8 \pm 1.0\mu$, respectively. Cystic thecal cells are significantly larger than precystic thecal cells. Secondary interstitial cell size is $11.3 \pm .3\mu$.

Electron Microscopic Identification of Thecal Cells

Three different procedures were used to localize thecal cells to healthy secondary follicles, atretic secondary follicles, precystic follicles or cystic follicles.

First, a light microscopic slide containing the same section as the electron microscopic grid was studied to identify the follicular structures present on the grid.

Secondly, at the electron microscopic level, the granulosa cells of the follicle in question were examined. The following characteristics provided the criteria for identification of the follicular structure being examined.

I. Granulosa cells of healthy secondary follicles are polyhedral in shape, and contain triangular or oval nuclei, evenly distributed ribosomes, oval mitochondria with lamellar cristae, smooth and rough endoplasmic reticulum, and Golgi complexes within their cytoplasm. The basal layer of granulosa cells are low columnar in appearance. All of the cells of the membrana granulosa are closely apposed. The underlying basement membrane appears intact.

II. Granulosa cells of atretic secondary follicles are often separated from each other, and are irregular in shape. This is especially true of the periantral cells. Nuclei are either oval or triangular, and either basally or centrally located. Often, the organelles are clumped around the nucleus, or at one pole of the cell. Cytoplasmic blebbing is often observed over the apical membrane of periantral cells. As well, lipid droplets normally seen only in the basal layers of the membrana granulosa of well developed secondary follicles (Peluso et al., 1980), are seen in scattered cells at all levels of the membrana. The basement membrane of these follicles appears normal.

III. The membrana granulosa of precystic follicles is very distinct. Its thickness is highly irregular. The cells are variable in shape, and cell boundaries often can not be distinguished. Nuclear shape is also highly irregular. Small indentations of the nucleus, not seen in granulosa cells of healthy or atretic follicles, are observed. Cytoplasmic blebbing is again observed over the apical membrane of scattered clusters of periantral granulosa cells. Organelles appear to be scattered throughout the cytoplasm of these cells. In contrast to atretic follicles, lipid droplets are observed

only in some of the granulosa cells, and almost exclusively within cells of the basal layer. In addition, numerous autophagic vacuoles are observed in granulosa cells of these precystic follicles. These are not observed in the membrana granulosa of any other follicle type studied (Figure 14).

IV. Three features of the membrana granulosa of a cyst distinguish this follicular type from the other three. First, it is the only case where the membrana granulosa consists of only a single layer of cells. Secondly, the nuclei of these cells are highly indented and irregular in shape, although the chromatin pattern is not disrupted. Thirdly, large, irregular intercellular spaces are frequently observed between the areas fused by junctional complexes of two adjacent granulosa cells. Occasionally, cytoplasmic extensions of two adjacent granulosa cells project into these spaces (Figure 15). The basal lamina underlying the cystic membrana granulosa appears hypertrophied in some areas, disrupted in some areas, and regular in others.

The final criteria used to localize thecal cells to a particular follicular type considers the morphological characteristics of the thecal cell itself.

Electron Microscopic Description of Thecal/Secondary Interstitial Cell Morphology

The theca interna of healthy secondary follicles contain fusiform-shaped steroidogenic cells interspersed between spindle-shaped fibroblasts and capillary endothelial cells. These cells contain spherical mitochondria with tubular or vesicular cristae, extensive smooth endoplasmic reticulum and lipid droplets (Figure 16). The thecal cells further from the basement membrane tend to contain much more lipid.

Nuclei are generally euchromatic, although the chromatin pattern in some nuclei is heterochromatic.

Thecal cells from atretic secondary follicles are morphologically similar to those of a healthy secondary follicle. However, atretic secondary follicular thecal cells are somewhat larger than those of a healthy secondary follicle, they contain more lipid and occasional autophagic vacuoles. The thecal ring surrounding these follicles appears to be more extensively vascularized, and the constituent cells form a disrupted layer (Figure 17). Nuclei in these cells are generally euchromatic.

Precystic and cystic thecal cells are very similar in morphology to each other. The size of these cells is similar to or larger than the size of thecal cells of atretic secondary follicles. They are polygonal in shape. Their cytoplasm contains primarily lipid droplets, mitochondria with tubulovesicular cristae, and smooth ER cisternae. An electron dense halo occasionally delineates the outer boundary of the lipid droplets in these cells (Figures 18a and b). The nuclei in precystic thecal cells are euchromatic, while nuclei in cystic thecal cells are heterochromatic.

Secondary interstitial cells are observed in clusters. Cell size within a single cluster is highly variable, as is cell shape. Generally, however, they are polygonal in shape. These cell profiles contain an abundance of lipid droplets of a wide variety of sizes, and mitochondria with tubulovesicular cristae. Nuclei are larger and euchromatic. These cells are easily distinguished as they occur in extensively vascularized clusters surrounded by connective tissue cells (Figure 19).

Electron Microscopic Analysis of Lipid Droplet Area

Lipid droplet area was measured in ten cells of each of the five cell types under study, from six different animals. Mean lipid droplet area ± S.E.M. is summarized in Figure 20.

The smallest lipid droplets are those within thecal cells from healthy secondary follicles (7.81 ± .54nm) and secondary interstitial cells (7.80 ± 1.61). Lipid droplets within these cells occupy approximately the same percentage of the cell profile area (43.14 ± 2.81% in healthy secondary thecal cells and 45.32 ± 5.83% in secondary interstitial cells). Mean lipid droplet area of precystic thecal cells is 8.62 ± 1.84 nm, lipid droplet area occupying 39.24% ± 4.40% of the total cell profile area. The mean area of lipid droplets within thecal cells of atretic secondary follicles is 12.82 ± .99 nm, and is significantly greater than the mean lipid droplet area of healthy and precystic follicular thecal cells and secondary interstitial cells ($p < .002$). The size of lipid droplets within cystic thecal cells is significantly larger ($p < .05$) than those within the other four classes of cells studied, with a mean area of 16.03 ± 2.90nm. However, the percentage of cystic thecal cell profile area occupied by lipid droplets (53.86 ± 8.05%) is not significantly different than the percentage of cell profile area occupied by lipid in the other four classes of cells examined in these ovaries.

Area of Mitochondrial Profiles

The area of mitochondrial profiles was measured in the same cells used in the analysis of lipid droplet area. Mean mitochondrial area $\pm$ S.E.M. is summarized in Figure 21.

Mean area of mitochondrial profiles within healthy secondary follicular thecal cells is 2.21 $\pm$ .32nm, accounting for 13.25 $\pm$ 1.81% of the mean cell profile area. Mitochondria within thecal cells of atretic secondary follicles are significantly smaller (1.54 $\pm$ .16nm) than mitochondria in thecal cells of healthy secondary, precystic and cystic follicular origin ($p<.05$). The percentage of atretic thecal cell profile area occupied by mitochondrial profiles (8.67 $\pm$ 1.12%) is also significantly smaller ($p < .03$) than the percentage of healthy secondary, precystic and secondary interstitial cell profile area occupied by mitochondrial profiles. Mean mitochondrial areas for precystic (1.83 $\pm$ .48nm) and cystic thecal cells (2.04 $\pm$ .74nm) are not significantly different. Mean mitochondrial areas expressed as a percentage of the total cell profile area are also similar (12.96 $\pm$ 1.18% and 12.05 $\pm$ 2.43%, respectively). The mean area of mitochondrial profiles within secondary interstitial cells is 1.96 $\pm$ .64nm and is not significantly different from the size of mitochondria within cells of the four classes of thecal cells examined. Mean mitochondrial profile area constitutes 11.24 $\pm$ 0.69% of the mean cell profile area.

Analysis of ^{125}I-hCG Binding Sites Using E.M. Radioautography

The specificity of the labelling of LH/hCG binding sites by ^{125}I-hCG was assessed in radioautographs of ovaries exposed to ^{125}I-hCG administered together with a 1,000 fold excess of unlabelled hormone. In contrast to ovaries exposed to the labelled hormone only, electron microscopic radioautographs of ovaries exposed to labelled and unlabelled hormone showed a negligible amount of labelling (0 grains/1,000μm surface length, or 1 grain/10^6μm surface length).

The number of LH binding sites per cell was assessed by counting the number of grains per cell on the same electron microscopic radioautographs used to assess lipid droplet and mitochondrial area. The number of ^{125}I-hCG positive sites are expressed per 1000μm surface length. The results (mean $\pm$ S.E.M.) are summarized in Figure 22.

The mean number of grains/1000μ on thecal cells from healthy secondary (12.1 $\pm$ 1.6) and atretic secondary follicles (7.7 $\pm$ 1.5) is not significantly different. Precystic thecal cells possess significantly fewer binding sites/1000μ (3.7 $\pm$ .7) as compared to healthy and atretic secondary follicular thecal cells ($p < .005$), as do cystic thecal cells (2.0 $\pm$ .7 receptors/1000μm, $p < .001$). The mean number of grains associated with secondary interstitial cells is 13.3 $\pm$ 1.4/1000μm, and is significantly greater than the number of grains associated with atretic, precystic and cystic thecal cells ($p < .006$), but is not significantly different than the number of sites associated with thecal cells of healthy secondary follicles.

E_2 Implanted Animals - Microcystic Ovarian Condition

Light Microscopic Analysis of Cell Size

A mean index of cell size of thecal cells from healthy secondary, atretic secondary and cystic follicles, as well as of secondary interstitial cells, is summarized in Figure 23.

Mean cell size of healthy secondary follicular thecal cells $\pm$ S.E.M. is 9.1 $\pm$ .4μ. Atretic secondary follicular thecal cells are significantly larger than those of a healthy secondary follicle ($p < .001$). The mean cell size is 11.4 $\pm$ .3μ. Mean cell size of thecal cells of cystic origin is 11.7 $\pm$ .4μ, ie. within the same size range as thecal cells from atretic secondary follicles. Secondary interstitial cell size is significantly larger than healthy and atretic follicular thecal cell size ($p < .05$), with a mean size of 12.2 $\pm$ .5μ.

Electron Microscopic Identification of Thecal Cells

The same three criteria used to localize thecal cells to either healthy secondary, atretic secondary and cystic follicles within the macrocystic ovary were employed here within the microcystic ovary. These included: 1) an evaluation of LM slides bearing the same section as the EM grids; 2) an examination of the granulosa cells of the follicle in question; and 3) the morphological characteristics of the thecal cell itself.

Granulosa cells within healthy and atretic follicles in the microcystic ovary are are identical to those from macrocystic ovaries. The membrana granulosa of microcystic follicles exhibit characteristics of granulosa cells from precystic follicles and

macrocysts. It consists of between one and four layers of highly irregular, dispersed cells. Nuclei are indented and irregular in shape, and they occupy most of the volume of the cell. The nuclear indentations, similar to those observed in precystic and macrocystic granulosa cells, are observed. Cytoplasmic extensions radiate from these cells, and are not restricted to the apical surfaces as they are in atretic and precystic granulosa cells. Organelles are scattered throughout the cytoplasm of these cells. Lipid droplets, seen in basal cells of the membrana granulosa of precystic follicles, are not observed here. Autophagic vacuoles, seen in precystic granulosa cells, are occasionally observed in these cells as well. Junctional complexes are rarely encountered (Figure 24).

Electron Microscopic Description of Thecal/Secondary Interstitial Cell Morphology

The morphology of thecal and secondary interstitial cells in microcystic ovaries does not appear to be different from the structure of analogous cells within macrocystic ovaries upon inspection. Ultrastructural differences between cells within the two different types of cystic ovaries becomes apparent only after quantitative analysis of lipid droplets and mitochondrial areas was complete. These differences will be discussed. Electron microscopic radioautographs of a microcystic thecal cell (Figure 25) and a secondary interstitial cell from an E_2-implanted ovary (Figure 26) are included for comparison.

Electron Microscopic Analysis of Lipid Droplet Area

Lipid droplet area was measured in ten cells of each cell type under study, from six different animals. Mean lipid droplet area $\pm$ S.E.M. is summarized in Figure 27.

The mean area $\pm$ S.E.M. of lipid droplets within healthy and atretic secondary follicular thecal cells and secondary interstitial cells is 8.33 $\pm$ .57nm, 9.82 $\pm$ 1.04, and 9.68 $\pm$ 1.04nm, respectively. There are no significant differences between these values. However, the percentages of cell profile area occupied by lipid droplets in healthy secondary thecal cells (52.61 $\pm$ 2.75%) and secondary interstitial cells (55.64 $\pm$ 3.46%) are significantly larger ($p < .03$) as compared to atretic secondary thecal cells (41.15 $\pm$ 3.40%). The mean area of lipid droplets in cystic thecal cells is 16.46 $\pm$ 98nm, and is significantly larger than for healthy secondary follicular thecal cells ($p < 0.006$), atretic secondary follicular theca ($p < 0.007$) and secondary interstitial cells ($p < 0.006$). The proportion of cystic thecal cell profile area occupied by lipid (63.50 $\pm$ 4.2%) is significantly greater compared to healthy and atretic secondary follicular thecal cells ($p < .04$).

Area of Mitochondrial Profiles

Area of mitochondrial profiles was measured in the same cells used in the analysis of lipid droplet area. Mean profile area $\pm$ S.E.M. for each of the four cell types examined is summarized in Figure 28.

Mean area of profiles within healthy secondary follicular thecal cells is 1.99 ± .16nm, or 11.15 ± 1.22% of the mean cell profile area. Mitochondrial profiles within thecal cells of atretic secondary follicles average 1.71 ± .15nm in area, or 9.76 ± 1.34% of the mean profile area of these cells. Cystic mitochondrial area is 1.84 ± .10nm, which corresponds to 8.27 ± 1.17% of the mean total profile area. The mean area of mitochondrial profiles within secondary interstitial cell is 2.26 ± .24nm, and is significantly larger than mitochondrial profiles of atretic and cystic follicular origin ($p < .04$). The large standard error for this cell population reflects the greater variability between these cells as compared to the other cell types. The percentage of the secondary interstitial cell profile area occupied by mitochondria is 10.40 ± 1.64%. There are no significant differences between the proportion of the total cell profile area occupied by mitochondrial profiles in these four cell types within a microcystic ovary.

Analysis of ^{125}I-hCG Binding Sites Using E.M. Radioautography

The number of LH/hCG binding sites per cell was assessed in the same manner as described for macrocystic ovaries, and is expressed per 1000μm surface length. The results (mean ± S.E.M.) are summarized in Figure 29.

Healthy secondary follicular thecal cells have an average of 8.1 ± 1.1 grains/1000μm. An average of 6.8 ± 1.0 grains/1000μm are associated with atretic secondary follicular thecal cells. Cystic thecal cells possess an average of .4 ± .3 LH/hCG sites/1000μm, which is significantly less than the number of sites on the three

other cell types examined in these ovaries ($p < .001$). Secondary interstitial cells have a significantly larger number ($16.1 \pm 2.4/1000\mu m$) of LH/hCG receptors as compared to atretic secondary and cystic thecal cells ($p < .004$), but not as compared to healthy secondary thecal cells. This may be due to the high standard error associated with grain counts for secondary interstitial cells.

Macrocystic vs. Microcystic Thecal and Secondary Interstitial Cells

A comparison of cell size, lipid droplet area, area of mitochondrial profiles and the number of ^{125}I-hCG binding sites/1000μm surface length between cells within macrocystic and microcystic ovaries was made in order to elucidate cellular differences in these two different polycystic ovarian conditions. These four parameters were assessed individually by statistically comparing measurements obtained for healthy follicular thecal cells. In those instances where the parameter under study was found to be the same in healthy secondary thecal cells from both macrocystic and microcystic ovaries, atretic thecal cell, cystic thecal cell and secondary interstitial cell values for the parameter were compared. The only parameter for which a significant difference was found between healthy secondary follicular thecal cells of macrocystic and microcystic ovarian origin is the number of ^{125}I-hCG binding sites/1000μm surface length, which was found to be significantly larger in healthy secondary thecal cells within EV-treated ovaries ($p < .04$). This may reflect differences in the specific activity of the ligand. It is more likely due to the fact that the endogenous LH levels in microcystic PCO are higher than in macrocystic PCO (McCarthy et al, 1986, Grosser et al., 1987; McCarthy and Brawer, 1989), while the same amount of ligand was administered in to animals of both models.

Cell size, lipid droplet area and mitochondrial profile area are similar in healthy secondary thecal cells of macrocystic and microcystic ovarian origin ($p > .60$) Because atretic follicles, cystic follicles and secondary interstitial cells all arise from the

different developmental pathways of a healthy secondary follicle (Erickson et al., 1985; Brawer et al., 1986), these three parameters can be compared in order to elucidate potential differences between macrocystic and microcystic ovaries.

Analysis of Cell Size

Atretic secondary thecal cells in macrocystic ovaries (12.20 $\pm$ .3μm) are significantly larger ($p < .05$) than those in microcystic ovaries (11.4 $\pm$ .3μm). Secondary interstitial cells within microcystic ovaries (12.2 $\pm$ .5μm) are significantly larger ($p < .03$) than the same cells from macrocystic ovaries (11.3 $\pm$ .3μm).

Lipid Droplet Area

There are no significant differences between the mean area of lipid droplet profiles or the percentage of mean cell profile area occupied by lipid in cells from macrocystic ovaries compared to their counterparts in microcystic ovaries.

Area of Mitochondrial Profiles

The mean area of mitochondrial profiles in macrocystic thecal cells (2.04 $\pm$ .74nm) is significantly larger than the mean profile area in microcystic thecal cells (1.84 $\pm$ .10nm). The percentage of the cell profile area occupied by mitochondrial profiles is also significantly larger in macrocystic thecal cells (12.05 $\pm$ 2.43% versus 8.27 $\pm$ 1.17%). Differences in mean mitochondrial profile area and in the percentage of secondary interstitial cell profile area occupied by mitochondria are not significant.

DISCUSSION

Alkaline Phosphatase Expression

Alkaline phosphatase is an enzyme important in reactions involving the synthesis of steroid hormones (Stafford et al., 1947). As well, it is believed to be necessary for the passage of steroids across cell membranes, as this process requires phosphate esterification (Moog, 1945). In the rat, alkaline phosphatase positive cells include follicular thecal cells, interfollicular stromal cells, secondary interstitial cells and vascular endothelial cells (Dempsey et al., 1949; Knigge and Leathem, 1954; McKay et al., 1961; Jacoby, 1962; Kent and Ryle, 1975). Granulosa cells are devoid of alkaline phosphatase activity (Knigge and Leathem, 1954; Kent and Ryle, 1975).

The expression of alkaline phosphatase appears to reflect tropic hormone stimulation and steroidogenesis in thecal cells and thecal derivatives (McKay et al., 1961; Pinkerton et al., 1961; Kent, 1974, Ross, 1974; Kent and Ryle, 1975). Administration of LH and hCG further enhances alkaline phosphatase activity in cells which are alkaline phosphatase positive (Kent and Ryle, 1975). The administration of powdered whole pituitary to hypophysectomized animals is followed by enhancement or restoration of alkaline phosphatase activity to developing follicles and newly formed corpora lutea, while corpora lutea in the ovary which were formed before hypophysectomy do not recover alkaline phosphatase activity (Dempsey et al., 1949). Hence, the alkaline phosphatase activity of a cell may also reflect its state of differentiation. In human ovaries, Dhom and Mende (1956) found alkaline

phosphatase activity in secondary interstitial cells to be inversely related to the lipid content of the cells, suggesting a possible correlation between alkaline phosphatase activity and fluctuations in hormone production. Thus, alkaline phosphatase is a valuable tool for assessing tropic hormone stimulation and steroidogenic activity in thecal cells and thecal derivatives in polycystic ovaries.

In the present study alkaline phosphatase activity, localized in control, macrocystic and microcystic ovaries using an immunohistochemical marker, is observed in thecal cells of healthy and atretic primary and secondary follicles, in corpora lutea (in control ovaries only), and in vascular endothelial cells. The relative expression of alkaline phosphatase in these structures is similar to that reported in the literature (Dempsey et al, 1949, Knigge and Leathem, 1954; McKay et al., 1961; and Kent and Ryle, 1975). The thecal wreath of macrocystic and microcystic follicles, in contrast to either primary or antral, healthy or atretic follicles and vascular endothelial cells, shows very little alkaline phosphatase activity and that which is present is primarily localized over capillary endothelial cells. This suggests that macrocystic and microcystic follicles are not steroidogenically active. Furthermore, the decrease in alkaline phosphatase expression in thecal cells of cystic follicles, as compared to that in atretic secondary follicles, may indicate that thecal cells in these two structures follow different pathways of differentiation, leading to different functional capacities.

Immunostaining of secondary interstitial cells for alkaline phosphatase is highly variable between control, EV-treated and E_2-implanted ovaries. Alkaline phosphatase

positive interstitial cell clusters in macrocystic ovaries are larger, more numerous, and more intensely stained than those in control ovaries. Thus, secondary interstitial cells in macrocystic ovaries may be either more sensitive to tropic hormone stimulation, more active in steroidogenesis than their counterpart in a cycling ovary, or both. Immunostaining of secondary interstitial cells in microcystic ovaries for alkaline phosphatase is localized to small, intensely stained strands of interstitial cells and to small, round, highly reactive cell clusters, neither of which are observed in control or macrocystic ovaries. These interstitial cells may possibly be derived from a spontaneously luteinized follicle, or from spontaneously luteinized, highly steroidogenic secondary interstitial cell clusters. As secondary interstitial cells normally arise from the thecal cell layer of collapsed atretic follicles (reviewed in Erickson, 1985), and as control and macrocystic ovaries do not contain secondary interstitial cell clusters that resemble those in the microcystic ovary in either morphology or alkaline phosphatase expression, it is possible that thecal cell precursors may follow a different pathway of cytodifferentiation in these E_2-treated ovaries, giving rise directly to ontogenically distinct, steroidogenically active secondary interstitial cells.

Cell Size and LH-Binding Capacity

Thecal cells and secondary interstitial cells are classified morphologically as either normal or hypertrophied. Hypertrophied cells are generally considered to be highly steroidogenic (Carithers and Green, 1972a,b; Erickson, 1985). Hypertrophy is one of the earliest changes in thecal cell morphology as atresia begins (Uilenbroek et

al., 1980). As atresia advances, a decrease in the number of tropic hormone receptors occurs (Uilenbroek et al., 1980). Richards and Midgley (1976) propose that follicular atresia is caused by a decrease in sensitivity of thecal cells to gonadotropic hormones (Richards and Midgley, 1976). After an atretic follicle collapses and its thecal cells are established as secondary interstitial cells, the number of tropic hormone receptors increases again, surpassing the number possessed by atretic follicular thecal cells (Shaha and Greenwald, 1982).

The capability of a cell to bind LH is considered to reflect tropic hormone sensitivity and to be an index of the steroidogenic capacity of thecal and secondary interstitial cells in the ovary (Dimmo, 1977; Dimmo and Berman, 1979; Rowe et al., 1981 and 1986). Classically, cell size and LH-binding capacity are considered to be valuable tools for assessing the steroid biosynthetic activity of thecal and secondary interstitial cells. Paradoxically, thecal hypertrophy and secondary interstitial cell formation in hypophysectomized rats are accompanied by an increase in the number of LH receptors and an increase in steroidogenic activity (Hillier and Ross, 1979; Erickson, 1981). In the present study, cell size and LH binding are evaluated in thecal and secondary interstitial cells in macrocystic and microcystic ovaries. A cell's size and its LH binding capacity will be evaluated in conjunction with alkaline phosphatase expression as an index of tropic hormone sensitivity and putative steroidogenic capacity. Cell size and LH binding characteristics alone will not be regarded as absolute indications of a cell's steroid biosynthetic activity.

In the macrocystic ovary, the size of atretic, precystic and cystic thecal cells and secondary interstitial cells is approximately the same. However the number of LH receptors per 1,000μm surface length, assessed using radioautography with ^{125}I-hCG as the ligand, is not the same. Secondary interstitial cells contain significantly more LH-binding sites than any of the other cells examined in this ovary, while precystic and cystic thecal cells contain significantly fewer binding sites than healthy or atretic follicular thecal cells and secondary interstitial cells. Thus, cell size in these ovaries does not appear to reflect tropic hormone sensitivity or putative steroidogenic activity. As precystic and cystic follicular thecal cells possess very few LH binding sites, one would predict that they are not LH sensitive and therefore are not likely actively synthesizing androgens. The minimal amounts of alkaline phosphatase in these cells also suggests this. Conversely, the large size of the cells, the vast number of LH binding sites, and the presence of alkaline phosphatase in secondary interstitial cells in macrocystic ovaries suggests that these cells are potentially very active in androgen synthesis.

In microcystic ovaries, secondary interstitial cells are significantly larger than healthy, atretic and cystic follicular thecal cells. They also possess significantly more LH binding sites. Thus, microcystic secondary interstitial cells appear to be highly sensitive to tropic hormone stimulation and thus potentially very actively steroidogenic. Alkaline phosphatase expression by these cells suggests the same. Despite the similarity in the size of atretic and microcystic thecal cells, the latter contain

significantly fewer LH receptor sites, paralleled by an appreciably smaller amount of alkaline phosphatase. Based on these observations, it appears that these hypertrophied cystic thecal cells are functionally distinct from atretic thecal cells, being less sensitive to tropic hormone stimulation and seemingly less androgenic. Perhaps they represent a terminal state of atresia

Mitochondrial and Lipid Droplet Profile Areas

Mitochondria provide a unique method for monitoring some of the temporal effects of gonadotropic hormones on ovarian steroidogenesis, as well as on the state of differentiation of follicular luteal tissue. LH stimulation of luteal and secondary interstitial cells from normally cycling ovaries result in mitochondrial changes. Structurally, mitochondria become more rounded in shape, and the cristae change from a lamellar to a tubulovesicular organization (Dimino et al., 1979; Rowe et al., 1981). These structural changes are accompanied by functional changes which involve the production of specific proteins important for steroidogenesis, including a cholesterol side chain cleavage complex which catalyses the rate limiting step in steroidogenesis (Omura et al., 1966; Rowe et al., 1986). This increase in protein synthesis is accompanied by an increased ability of mitochondria to convert pregnenolone to progesterone (Dimino et al., 1979; Dimino and Berman, 1979; Rowe et al., 1981 and 1986). Mitochondrial steroidogenic activity increases with follicular development (Dimino, 1977; Rowe et al., 1981), a process which is paralleled by further cytodifferentiation of thecal cells (reviewed in Erickson, 1985).

Removal of LH stimulation of the ovary by hypophysectomy results in a reduction in size, number of mitochondria and the number of cristae in mitochondria. Furthermore, mitochondrial cristae are restructured from a tubulovesicular to a lamellar organization during the first month following hypophysectomy (Carithers and Green, 1972a). As well, the amount of lipid contained within secondary interstitial cells increases appreciably following hypophysectomy (Carithers and Green, 1972a,b). As mitochondria and lipid droplets are both involved in steroid synthesis, and as the size of both is affected by LH, mitochondrial and lipid droplet area are assessed in the present study to provide an additional index of tropic hormone stimulation and steroidogenic capacity of thecal and secondary interstitial cells within polycystic ovaries.

Healthy, atretic, precystic and cystic follicular thecal cells and secondary interstitial cells within macrocystic ovaries all contain mitochondria with tubulovesicular cristae. The area of mitochondrial profiles in atretic follicular thecal cells is significantly smaller than mitochondria within thecal cells of healthy, precystic and cystic origin. The proportion of the cell profile area occupied by mitochondrial profiles is significantly smaller in these cells as well, suggesting that they also possess fewer mitochondria than healthy thecal, precystic thecal, cystic thecal and secondary interstitial cells. These atretic follicular thecal cells also contain larger lipid droplets than healthy and precystic thecal cells. Based on the reports of Carithers and Green (1972a,b), the number and size of mitochondria and the size of lipid droplets in these atretic follicular thecal cells do not fit the typical profile of a LH-stimulated,

androgenic ovarian cell, as the number of LH binding sites and alkaline phosphatase expression suggest that they are sensitive to tropic hormone stimulation and are androgenic. Mitochondrial and lipid droplet indices in these cells, relative to other thecal cells in this ovary, suggest however that these cells could be partially deactivated ie. on the path to inactivity, while cystic thecal cells may represent the completion of the process..

Macrocystic follicles, in marked contrast to atretic thecal cells in EV-treated ovaries, possess negligible amounts of alkaline phosphatase activity and very few LH binding sites. They also contain the largest lipid droplets. These indices together support the alkaline phosphatase data indicating that macrocystic thecal cells are steroidogenically inactive. Furthermore, they indicate that macrocystic thecal cells are functionally and ultrastructurally distinct from atretic follicular thecal cells.

In microcystic ovaries, the largest mitochondria are found in secondary interstitial cells. However, the proportion of the total cell profile area occupied by mitochondrial profiles is relatively constant between the four cell types examined. Nonetheless, alkaline phosphatase expression, the capacity to bind LH, cell size, mitochondrial size and ultrastructural organization all suggest that these cells are synthetically active and that they probably contribute substantially to the plasma steroid hormone profile in these animals.

Cystic thecal cells contain significantly larger lipid droplets than healthy thecal, atretic thecal, and secondary interstitial cells. In addition, a significantly larger

proportion of the cell profile area in microcystic thecal cells is occupied by lipid. Alkaline phosphatase activity and LH-sensitivity are minimal in these cells. These observations, together with the abundance of lipid, suggest that as was the case for macrocystic thecal cells, microcystic thecal cells are not steroidogenic. The tubular organization of mitochondrial cristae in these cells, as in macrocystic thecal cells, again suggests that they are not terminally deactivated.

How are cysts related to other follicular structures?

The morphology of the follicular structures in EV-treated and E_2-implanted polycystic ovaries show signs of atresia. The changes in follicular dynamics preceding the development of the polycystic morphology suggest that cyst formation is a consequence of an alteration or arrest of the atretic process (Brawer et al., 1986, 1989). The morphology of precystic follicles, as well as the LH-binding capacity and degree of alkaline phosphatase expression, which are intermediate between atretic and cystic follicular characteristics, support this. As well, the membrana granulosa of precystic follicles is characteristic of a follicle in an advanced state of atresia (Zeller, 1984), containing lipid droplets in the perimural layer, exhibiting a disruption of junctional complexes and showing cytoplasmic blebbing of the apical surfaces of the periantral layer of cells. The membrana granulosa of a macrocyst is distinct from that of an atretic or precystic follicle and, although the cells are irregular and not functional, they do appear to be stable.

The transition from the precystic to the cystic condition coincides with a loss

of hCG binding sites and, presumably, a loss in sensitivity to LH. This loss of LH binding sites likely results in a diminution in androgen production. The lack of alkaline phosphatase activity and the abundance of lipid in these cells lends support to this idea. As excessive local concentrations of androgen appear to be instrumental in marking specific follicles for atresia (Louvet et al., 1975), an attenuation in local androgen concentrations in these follicles may result in an arrest of the atretic process and the stabilization of the affected follicle as a relatively inert cyst which, because of its large size, is unable to collapse.

Microcystic thecal cells also show minimal alkaline phosphatase activity and a few LH binding sites, as do macrocystic thecal cells. The membrana granulosa of a microcystic follicle is not identical to that of a macrocyst, but rather possesses characteristics of the membrana granulosa of both precystic and macrocystic follicles. Differences between the morphology of microcystic and macrocystic follicles detailed in this paper, as well as the size of the microcystic follicle raise the question as to whether or not it is possible that the microcystic follicle is merely an atretic follicle prior to collapse. Further studies are required to determine this. As some secondary interstitial cell clusters exhibit the approximate shape and size of microcystic follicles, and as microcystic follicles still bear a resemblance to atretic follicles, it is possible that microcystic follicles are merely degenerating follicles which follow a different atretic pathway, but to the same end, ie. to become a secondary interstitial cell cluster. Secondary interstitial cells are far more numerous in these E_2-implanted ovaries, as

compared to EV-treated ovaries. The collapse of microcysts and the persistence of macrocysts may account for this in part.

On the basis of morphology, the number of LH receptors, and the number of cells which contain large quantities of alkaline phosphatase, one would predict that the polycystic ovary in the E_2-implanted rat is far more active in synthesizing androgens than is its counterpart in the EV-treated model. If local and circulating androgen levels are in fact higher in E_2-implanted rats with PCO, this would have important consequences on pituitary function and on the expression of secondary sex characteristics in these rats. This, however, remains to be determined.

REFERENCES

Adams, J., D.W. Polson, N. Abdulwahid, D. Morris, S. Franks, H.D. Mason, M. Tucker and J. Price. Multifollicular ovaries: clinical and endocrine features and response to pulsatile gonadotropin releasing hormone. Lancet **II**:1375, 1985.

Adams, J., D.W Polson, S Franks. Prevalence of polycystic ovaries in women with anovulation and idiopathic hirsutism. British Medical Journal **293**:353, 1986.

Aschem, P. Aging in the hypothalamic-hypophyseal-ovarian axis in the rat. In: Hypothalamus, Pituitary and Aging (A Everill and J.A. Burgess, eds.). Springfield, IL: Charles C Thomas. pp. 376-418, 1976.

Bahl, O.P. Human chorionic gonadotropin: amino acid sequence of the alpha and beta subunits Biochem. Biophys. Research Communications **48**:146, 1972.

Blake, C A., R.J. Scaramuzzi, J Hilliard and C H. Sawyer. Circulating levels of pituitary gonadotropins and ovarian steroids in rats after hypothalamic deafferentation. Neuroendocrinology **12**:86, 1973.

Blake, C., R. Weiner, R. Gorski and G Sawyer. Secretion of pituitary luteinizing hormone and follicle stimulating hormone in female rats made persistently estrous or diestrous by hypothalamic deafferentation. Endocrinology **90**:855, 1972

Bortolussi, M., G. Marini and A. Dal Lago. Autoradiographic study of the distribution of LH receptors in the ovary of untreated and gonadotropin primed immature rats Cell and tissue research **183**:329, 1977

Bortolussi, M., G. Marini and M L. Relon. A histochemical study of the binding of I^{125} hCG to the rat ovary throughout the estrous cycle. Cell and tissue research 197:213, 1979

Bortolussi, M., G. Marini, M.T. Rolandi and L. Colombo. In vitro binding of I^{125} hCG to the rat ovary from birth to puberty. Cell and tissue research **214**:633, 1981.

Brachet, J. The localization and role of ribonucleic acid in the cell. Annual of the New York Academy of Science **50**:861, 1950.

Brawer, J.R., F. Naftolin, J. Martin and C. Sonneschein. Effects of a single injection of Estradiol Valerate on the hypothalamic arcuate nucleus and on reproductive function in the female rat. Endocrinology 103:501, 1978.

Brawer, J.R., H. Schipper and F. Naftolin Ovary-dependent degeneration in the hypothalamic arcuate nucleus. Endocrinology 107:274, 1980.

Brawer, J.R., H. Schipper and B. Robaire. Effects of long term androgen and estradiol exposure on the hypothalamus. Endocrinology 112:194, 1983.

Brawer, J.R., M. Munoz and R. Farookhi Development of the polycystic ovarian condition (PCO) in the estradiol-valerate treated rat. Biology of Reproduction 35:647, 1986.

Brawer, J.R., M. Richard and R. Farookhi. Pattern of human chorionic gonadotropin (hCG) binding in the polycystic ovary. American Journal of Obstetrics and Gynecology (in press), 1989.

Butcher, R.L., W.E Collins and N.W. Fugo. Plasma concentrations of LH, FSH, prolactin, progesterone and estradiol 17-beta throughout the 4-day estrous cycle of the rat. Endocrinology 94:1704, 1974.

Byskov, A.G. Follicular Atresia. In: The Vertebrate Ovary (R.E. Jones, Ed). New York. Plenum Press, pp. 533-562, 1978.

Byskov, A.G. Atresia. In: Ovarian Follicular Development and Function (A.R. Midgley and W A. Sadley, eds.). New York: Raven Press pp 41-57

Campbell, C.S. and N.B. Schwartz. The impact of constant light on the estrous cycle of the rat Endocrinology 106:1230, 1980.

Carithers, J.R. and J A. Green. Ultrastructure of rat ovarian interstitial cells. I Normal structure and regressive changes following hypophysectomy Journal of Ultrastructural Research 39:239, 1972a.

Carithers, J.R. and J.A. Green. Ultrastructure of rat ovarian interstitial cells II. Response to gonadotropin. Journal of Ultrastructural Research 39:251, 1972b.

Carriere, P.D., J.R. Brawer and R. Farookhi. Pituitary gonadotropin-releasing hormone receptor content in rats with polycystic ovaries. Biology of Reproduction 38:562, 1988.

Carriere, P., R. Farookhi and J.R. Brawer. The role of aberrant hypothalamic opiatergic function in generating polycystic ovaries in the rat. Canadian Journal of Physiology and Pharmacology (in press), 1989.

Convery, M.M., G.F. McCarthy and J.R. Brawer. Remission of the polycystic ovarian condition (PCO) in the rat following hemiovariectomy. Anatomical Record (in press) 1989.

Copmann, T.L. and W.C. Adams. Relationship of polycystic ovarian induction to prolactin secretion: prevention of cyst formation by bromocriptine in the rat. Endocrinology 108:1095, 1981.

Culler, M.D. and A. Negro-Villar. Pulsatile follicle-stimulating hormone secretion is independent of luteinizing-hormone releasing hormone (LHRH): pulsatile replacement of LHRH bioactivity in LHRH-immunoneutralized rats. Endocrinology 120:2011, 1987.

Daane, T.A. and A.F. Parlow. Serum FSH and LH in constant light-induced persistent estrus: short-term and long-term studies. Endocrinology 88:964, 1971.

Dawson, A.B. and M. McCabe. The interstitial tissue of the ovary in intact and juvenile rats. Journal of Morphology 88:543, 1951.

Deane, H.W. Histochemical characterizations of atretic follicles in the rat's ovaries. Anatomical Record 111:504 (Abstract), 1951.

Deane, H.W. Histochemical observations on the ovary and oviduct of the albino rat during the estrous cycle. American Journal of Anatomy 91:363, 1952.

Deanesly, R. Origins and development of interstitial tissue in ovaries of rabbit and guinea-pig. Journal of Anatomy 113:251, 1972.

Dempsey, E.W., R.O. Greep and H.W. Deane. Changes in the distribution and concentration of alkaline phosphatases in tissues of the rat after hypophysectomy or gonadectomy and after replacement therapy. Endocrinology 44:88, 1949.

Dhom, G. and H.J. Mende. Die alkalische phosphatase in den hiluszellen des ovars. Virchow's Arch. 328:337, 1956.

Diersche, D., A.N. Battacharya, L.E. Atkinson and E. Knobil. Circhoral oscillations of plasma LH levels in the ovariectomized rhesus monkey. Endocrinology 87:850, 1970.

Dimino, M.J. Differences in mitochondrial steroidogenesis between follicular and luteal tissues of porcine ovaries. Endocrinology 101:1844, 1977.

Dimino, M.J. and K. Berman. Increases in mitochondrial steroidogenesis after short term incubation of porcine ovarian follicles with luteinizing hormone. Endocrinology 104:780, 1979.

Dufau, M.L., K.J. Catt and T. Tsuruhara. Biological activity of human chorionic gonadotropin released from testis binding sites. Proceedings of the National Academy of Science 69:2414, 1972.

Engel, L.L. The biosynthesis of estrogens. In: Handbook of Physiology-Endocrinology II, Part I (R.O Greep, ed.). Baltimore, Maryland. Waverly Press, pp. 467, 1973.

Erickson, G.F. Primary cultures of ovarian cells in serum-free medium as models of hormone-dependent differentiation. Molecular and Cellular Endocrinology 29:21, 1983

Erickson, G.F., D.A Magoffin, C.A. Dyer and C Hofeditz The ovarian androgen producing cells: a review of structure/function relationships Endocrine Reviews 6(3):371, 1985.

Eshkol, A. and B Lunenfeld. Gonadotropic regulation of ovarian development in mice during infancy. In: Gonadotropins (B B. Saxena, C.G Beling and H M Grandy, eds.) New York. John Wiley and Sons, Inc., pp 335-346 1972

Farookhi, R., R Hemmings and J R Brawer Unilateral ovariectomy restores ovulatory cyclicity in rats with a polycystic ovarian condition Biology of Reproduction 32:530, 1985

Fawcett, D.W., J.A. Long and A L. Jones. The ultrastructure of the endocrine glands Recent Progress in Hormone Research 25:315, 1969

Fink, G. Feedback actions of target hormones on the hypothalamus and pituitary with special reference to gonadal steroids. Annual Review of Physiology 41:571, 1979

Ford, D.H. and A. Hirschman. Alkaline Phosphatase activity in the ovaries of immature and maturing albino rats. Anatomical Record 121:531, 1955

Fortune, J.E. and D.R. Armstrong. Hormonal control of 17-beta-estradiol biosynthesis in proestrous rat follicles: estradiol production by isolated theca versus granulosa. Endocrinology **102**:227, 1978.

Franchmont, P. A study of the cross-reaction between human chorionic gonadotropin and pituitary luteinizing hormones (hCG and hCG). European Journal of Clinical Investigation **1**:65, 1970.

Gallo, R.V. and A. Bona-Gallo. Lack of ovarian steroid negative feedback on pulsatile luteinizing hormone releasing hormone between estrous and diestrous day 1 in the rat estrous cycle. Endocrinology **116**:1525, 1985.

Goldzieher, J.W. and L.R. Axelrod. Clinical and biochemical features of polycystic ovarian disease. Fertility and Sterility **14**:631, 1963.

Goldzieher, J.W. Polycystic ovarian disease. Fertility and Sterility **35**:371, 1981.

Gorski, R.A. Gonadal hormones and the perinatal development of neuroendocrine function. In Frontiers in Neuroendocrinology (L. Martini and W.F. Ganong, eds.) New York: Oxford University Press. pp. 237-290. 1969.

Grosser, P.M., G.F. McCarthy, B. Robaire, R. Farookhi and J.R. Brawer. Plasma patterns of LH, FSH and prolactin in rats with a polycystic ovarian condition induced by estradiol valerate. Endocrinology **44**:33, 1987.

Guraya, S.S. and G.S. Greenwald. A comparative histochemical study of interstitial tissue and follicular atresia in the mammalian ovary. Anatomical Record **149**:411, 1968.

Hahn, D.W. and J.I. McGuire. The androgen sterilized rat: induction of ovulation and implantation by luteinizing hormone releasing hormone. Endocrinology **102**:1741, 1978.

Halasz, B. The endocrine effects of isolation of the hypothalamus from the rest of the brain. In Frontiers in Neuroendocrinology (L. Martini and W.F. Ganong, eds.). New York: Oxford University Press. p. 307, 1969.

Han, S.S., H.J. Rajaniemi, M.I. Cho, A.N. Hirshfield and A.R. Midgley Jr. Gonadotropin receptors in rat ovarian tissue. II. Subcellular localization of LH binding sites by EM radioautography. Endocrinology **95**:589, 1974.

Hemmings, R., R. Farookhi and J.R. Brawer. Pituitary and ovarian responses to luteinizing hormone releasing hormone in a rat with polycystic ovaries. Biology of Reproduction **29**:239, 1983

Hillier, S.G. and G.T. Ross. Effects of exogenous testosterone on ovarian weight, follicular morphology and intraovarian progesterone concentration in estrogen-primed hypophysectomized immature female rats. Biology of Reproduction **20**:261, 1979.

Ireland, J.J. and J.S. Richards. A previously undescribed role for luteinizing hormone (LH:hCG) on follicular cell differentiation. Endocrinology **102**:1458, 1978.

Jacoby, F. Ovarian Histochemistry. In: The Ovary, Volume 1 (S. Zuckerman, Ed.) New York: Academic Press, pp. 189-245, 1962

Kammerman, S. and R.E. Canfield. The inhibition of binding of iodinated human chorionic gonadotropin to mouse ovary in vitro. Endocrinology **90**:384, 1972

Kammerman, S., C.E. Canfield, J. Kolena and C.P. Channing. The binding of iodinated hCG to porcine granulosa cells. Endocrinology **91**:65, 1972

Karnovsky, M.J. A formaldehyde-glutaraldehyde fixative of high osmolarity for use in, - electron microscopy. Journal of Cell Biology **27**:137a, 1965

Karnovsky, M.J. Use of ferrocyanide-reduced osmium tetroxide in electron microscopy. Proceedings of the 14th Annual Meeting of the American Society of Cell Biology, **11**:146, 1971

Kawakami, M. and S. Visessuvan. The differing responsiveness of the anterior and middle-anterior hypothalamic area to estradiol benzoate implant inhibition of compensatory ovarian hypertrophy. Endocrinology **74**:271, 1979

Kingsbury, B.F. Atresia and the interstitial cells of the ovary. American Journal of Anatomy 65:309, 1939

Kent, J. Some histochemical changes in immature mouse ovaries after gonadotropin treatment. Journal of Endocrinology **61**:xxi, 1974.

Kent, J. and M. Ryle. Histochemical studies on three gonadotropin-responsive enzymes in the infantile mouse ovary. Journal of Reproduction and Fertility **42**:519, 1975.

Khoury, S.A., N.E. Reame, R. Kelch and J.C. Marshall Diurnal patterns of pulsatile luteinizing hormone secretion in hypothalamic amenorrhea: reproducibility and responses to opiate blockade and an alpha-adrenergic agonist. Journal of Clinical Endocrinology and Metabolism **64**:755, 1987.

Knigge, K. and J Leatham. Growth and atresia of follicles in the ovary of the hamster. Anatomical Record **124**:679, 1954.

Knobil, E. The neuroendocrine control of the menstrual cycle. Recent Progress in Hormone Research **36**:53, 1980

Koch, Y., V. Zor, P Chobsieng et al. Binding of luteinizing hormone and human chorionic gonadotropin to ovarian cells and activation of adenylate cyclase. New England Journal of Medicine **291**:179, 1974.

Kopriwa, Beatrix M A comparison of various procedures for fine grain development in electron microscopic radioautography. Histochemistry **44**:201-224, 1975.

Kopriwa, B M, G M Levine and N J. Nadler. Assessment of resolution by half distance values for tritium and radioiodine in electron microscopic radioautographs using Ilford L4 emulsion developed by "sodium physical" or D-19b methods Histochemistry **80**:519, 1984

Lee, C Y and R.J. Ryan The centrifugal fractionation of I^{125} labelled human luteinizing hormone (HLH) accumulated by rat ovarian slices. In: Protein and Polypeptide Hormones (M Margoulies and F.C. Greenwood, eds.) Exerpta Medica, Amsterdam p. 513, 1972a.

Lee, C Y and R J. Ryan. Luteinizing hormone receptors. Specific binding of human LH to homogenates of luteinized rat ovaries Proceedings of the National Academy of Science **69**:3520, 1972b

Leidenberger, F and L.E. Reichert, Jr. Evaluation of a rat testis homogenate radioligand receptor assay for human pituitary LH. Endocrinology **90**:384, 1972.

Louvet, J P., S.M Harman, J.R. Schreiber and G T. Ross. Evidence for a role of androgens in follicular maturation. Endocrinology **97**:366, 1975.

Lunenfield, B. and A. Eshkol. Immunology of human chorionic gonadotropin (hCG). Vit. Hormone 25:137, 1967.

McCarthy, G.F., J.R. Brawer and R. Farookhi. Plasma LH patterns characterizing the development of the polycystic ovarian condition (PCO) in the estradiol valerate (EV)-treated rat. Biology of Reproduction **34 (suppl. 1)**:153, 1986.

McCarthy, G.F., R. Farookhi and J.R Brawer Polycystic ovaries (PCO) occur in response to a specific pulsatile pattern of luteinizing hormone (LH). Biology of Reproduction **36 (suppl. 1)**:172, 1987.

McCarthy, G.F. and J.R. Brawer. Induction of a Stein-Leventhal type polycystic ovarian condition (PCO) in the rat: a new model for cystic ovarian disease (Submitted), 1989.

McEwen, B.S. Steroid hormone interactions with the brain, cellular and molecular aspects. In Reviews of Neuroscience (D.M Schneider, Ed.) New York Raven Press, pp. 1-30 1979.

McKay, D.G., J.H M. Pinkerton, A F. Hertig and S Danziger. The adult human ovary: a histochemical study. Obstetrics and Gynecology **18**:13, 1961

McNatty, K P, A Makris, G. DeGrazia, R Osathanodh, and K J. Ryan. The production of progesterone, androgens and estrogens by granulosa cells, thecal tissue and stromal tissue from human ovaries in vitro Journal of Clinical Endocrinology and Metabolism **49**:687, 1979.

Mahesh, V.B. Current concepts of the pathophysiology of the polycystic ovary syndrome. In. Endocrine Physiopathology of the Ovary (R I. Tozzini, G Reeves and R L. Pineda, eds.). Amsterdam: Elsevier/North-Holland Biomedical Press. pp. 275-294. 1980.

Mahesh, V.B. and R B. Greenblatt. Steroid secretions of the normal and polycystic ovary. Recent Progress in Hormone Research **20**:341, 1964

Malone, T E: Observations on the histochemical localization of alkaline glycerophosphatase in developing corpora lutea of albino rats American Journal of Anatomy **106**:41, 1960

Matuso, H., Y. Baba, R.M G. Nair, A Arimura and A V. Schally Structure of the porcine LH and FSH releasing hormone The proposed amino acid sequence Biophysiology Research Communications **43**:1344, 1971.

Al-Mehdi, M.I.H. Fine structure and origin of interstitial tissue in the ovary of the pregnant rat. Acta Anatomica **103**:245, 1979.

Meyer, R.K. and W H McShan. Enzymes in the Ovarian Tissues of Rats. In: Menstruation and its Disorders (Earl Engle, Ed.). Springfield, IL: C.C. Thomas, pp. 62-95, 1950.

Midgley, A.R. Radioimmunoassay: a method for human chorionic gonadotropin and human luteinizing hormone. Endocrinology **79**:10, 1966.

Midgley, A.R. Autoradiographic analysis of gonadotropin binding to rat ovarian tissue sections Advances in Experimental Medical Biology **36**:365, 1973.

Midgley, A.R , A J Zeleznik, J.S Richards and S.S. Han. Gonadotropin and estradiol receptors and follicular development. In: Advances in Fertility Regulation through Basic Research (W A. Sadler and S Segal, eds.). 1974.

Mobbs, C.V., K Flurkey, D.M Gee, K Yamamoto, Y.N. Sinha and C.E. Finch. Estradiol-induced adult anovulatory syndrome in female C57bl/6j mice: age-like neuroendocrine, but not ovarian, impairments. Biology of Reproduction **30**:556, 1984

Morgan, F.J. and R E. Canfield. Nature of the subunits of human chorionic gonadotropin. Endocrinology **88**:1045, 1971.

Morgan, F.J., R.E Canfield, J.L. Vaitukaitis, and G.T. Ross. Properties of the subunits of human chorionic gonadotropin. Endocrinology **94**:1601, 1974.

Mori, H. and K. Matsumoto. Development of the secondary interstitial gland in the rabbit ovary Journal of Anatomy **116**:417, 1973

Nimrod, A., G F Erickson and K.J. Ryan. A specific FSH receptor in rat granulosa cells: properties of binding *in vitro* Endocrinology **98**:56, 1974.

Omura, T., E. Sanders, R.W. Estabrook, D.Y. Cooper and O. Rosenthal. Isolation from adrenal cortex of a nonheme iron protein and a flavoprotein functional as a reduced triphosphopyridine nucleotide-cytochrome P-450 reductase. Archives of Biochemistry and Biophysiology **138**:164-180, 1966.

Parker, C.R. and V.B. Mahesh. Interrelationship between excessive levels of circulating androgens in blood and ovulatory failure. Journal of Reproductive Medicine **17**:75, 1976.

Payne, R.W., A.A. Hellbaum and J.N. Owens. The effect of androgens on the ovaries and uterus of the estrogen treated hypophysectomized immature rat. Endocrinology **59**:306, 1956.

Payne, R.W. and R.H. Runser. The influence of estrogen and androgen on the ovarian response of hypophysectomized immature rats to gonadotropins. Endocrinology **62**:313, 1958

Pederson, T. Follicle kinetics in the ovary of the cyclic mouse. Acta Endocrinologica **64**:304, 1970.

Peluso, J.J., C. England-Charlesworth D.L. Bolender and R.W. Steger. Ultrastructural alterations associated with the initiation of follicular atresia. Cell and Tissue Research **211**:105, 1980.

Peters, H. The development of the mouse ovary from birth to maturity. Acta Endocrinologica **62**:98, 1969

Pinkerton, J H.M, D.G. McKay and E.C. Adams. Development of the human ovary - a study using histochemical techniques. Obstetrics and Gynecology **18**:152, 1961

Ponder, B A and M.M Wilkinson. Inhibition of endogenous tissue alkaline phosphatase conjugates in immunohistochemistry Journal of Histochemistry and Cytochemistry **29**:981, 1981.

Popkin, R.M., H.M. Fraser and R.G. Gosden Effects of LHRH-antagonist on LHRH immunoneutralization on pituitary and ovarian LHRH receptors in female rats. Journal of Reproduction and Fertility **69**:245, 1983.

Rajaniemi, J. and T. Vanha-Perttula. Specific receptor for LH in the ovary, evidence by radioautography and tissue fractionation Endocrinology **90**:1, 1972

Rajaniemi, J.H., A.R. Midgley, J.A. Duncan and L.E. Reichert. Gonadotropin receptors in rat ovarian tissue. III. Binding sites for luteinizing hormone and differentiation of granulosa cells to luteal cells. Endocrinology **101**:898, 1977.

Rajaniemi, J.H., A.N. Hirshfield and A.R. Midgley Jr. Gonadotropin receptors in rat ovarian tissue. I. Localization of LH binding sites by fractionation of subcellular organelles. Endocrinology **95**:579, 1974.

Ramey, J.W., R.F. Highsmith, W.W. Wilfinger and D.M. Baldwin. The effects of gonadotropin-releasing hormone and estradiol on luteinizing hormone biosynthesis in cultured rat anterior pituitary cells. Endocrinology **120**:1503, 1987.

Rebar, R.W., H.L. Judd, S.S.C. Yen, J. Rakoff, G. Brandenberg and F. Naftolin. Characterization of the inappropriate gonadotropin secretion in polycystic ovary syndrome. Journal of Clinical Investigation 57:1320, 1976.

Rennels, E.G. Influence of hormones on the histochemistry of ovarian interstitial tissue in the immature rat. American Journal of Antomy **88**:63, 1951.

Rice, B.F. and K. Savard. Steroid hormone formation in the human ovary. IV: Ovarian stromal compartment: formation of radioactive steroids from acetate-1-^{14}C and action of gonadotropins. Journal of Clinical Endocrinology and Metabolism 26:593, 1966.

Richard, Martine. Localization of LH/hCG binding sites in the polycystic ovary. A thesis submitted to the Faculty of graduate Studies and Research in partial fulfillment of the requirements for the degree of Master of Science, McGill University, Montreal. October 1988.

Richards, J.S., J.J. Ireland, M.C. Rao, G.A. Bernath, A.R. Midgley and L.E. Reichert. Ovarian follicular development in the rat: hormone receptor regulation by estradiol, follicle stimulating hormone and luteinizing hormone. Endocrinology **99**:1562, 1976.

Richards, J.S. and A.R. Midgley. Protein hormonal action: a key to understanding ovarian follicular and luteal cell development. Biology of Reproduction **14**:82, 1976.

Robaire, B., L.L. Ewing, D.C. Irby and C. Desjardins. Interactions of testosterone and estradiol 17-ß on the reproductive tract of the male rat. Biology of Reproduction 21:455, 1979.

Robaire, B. and B.F. Hales. Regulation of epididymal glutathione S-transferases: effects on orchidectomy and androgen replacement. Biology of Reproduction 26:559-565 1982.

Ross, G.T. Gonadotropins and preantral follicular maturation in women. Fertility and Sterility 25(6):522, 1974.

Rowe, M.J., R.R. Bieszczad, M.A. Neymark and M.J. Dimino. Synthesis of Mitochondrial proteins after stimulation of ovarian follicles by luteinizing hormone. Endocrinology 108:127, 1981.

Rowe, M.J. and J.L. Hopko. Luteinization-specific ovarian mitochondrial proteins. Biology of Reproduction 35:906, 1986.

Ryan, K.J. and O.W. Smith. Biogenesis of estrogens by the human ovary. IV. Formation of neutral steroid intermediates. Journal of Biological Chemistry 236:2207, 1961.

Ryan, K.J. and Z. Petro. Steroid biosynthesis by human ovarian granulosa and thecal cells. Journal of Clinical Endocrinology and Metabolism 26:46, 1966.

Ryan, R.J. and C.Y. Lee. The role of membrane bound receptors. Biology of Reproduction 14:16, 1976.

Schulster, A., R. Farookhi and J.R. Brawer. Polycystic ovarian condition in estradiol-valerate treated rats: spontaneous changes in characteristic endocrine features. Biology of Reproduction 31:587, 1984.

Schwall, R. and G.F. Erickson. Functional and morphological changes in rat theca cells during atresia. In: Dynamics of Ovarian Function (W.B. Schwartz and Hunzicker-Dunn, eds.). Raven Press, NY. p. 29. 1981.

Shaha, C. and G.S. Greenwald. Autoradiographic analysis of changes in ovarian binding of FSH and hCG during induced follicular atresia in the hamster. Journal of Reproduction and Fertility 66:197, 1982.

Simard, M., J.R. Brawer and R. Farookhi. An intractable, ovary-independent impairment in hypothalamo-pituitary function in the estradiol valerate-induced polycystic ovarian condition in the rat. Biology of Reproduction 36:1229, 1987.

Stafford, R.O., W.H. McShan and R.E. Meyer. Acid and alkaline phosphatases in ovarian tissues of the rat during pregnancy and lactation. Endocrinology 41:45, 1947.

Stratton, L.G., L.L. Ewing, D.C. Irby and C. Desjardins. Efficacy of testosterone-filled polydimethyl-siloxane implants in maintaining plasma testosterone in rabbits. Journal of Reproduction and Fertility 35:235, 1973.

Uilenbroek, J. Th. J. and J.S. Richards. Ovarian follicular development during the rat estrous cycle: gonadotropin receptors and follicular responsiveness. Biology of Reproduction 20:1159, 1979.

Uilenbroek, J. Th. J., P.J.A. Woutersen and P. Van der Schoot. Atresia of preovulatory follicles: Gonadotropin binding and steroidogenic activity. Biology of Reproduction 23:219, 1980.

Vitale, R., D.W. Fawcett and M. Dym. The normal development of the blood-testis barrier and the effects of clomiphene and estrogen treatment. Anatomical Record 176:333, 1973.

Waldstreicher, J., N.F. Santoro, J.E. Hall, M. Filicori and W.F. Crowley. Hyperfunction of the hypothalamic-pituitary axis in women with polycystic ovarian disease: indirect evidence for partial gonadotropin desensitization. Journal of Clinical Endocrinology and Metabolism 66:165, 1988.

Wildt, L. and G. Leyendecker. Induction of ovulation by chronic administration of naltrexone in hypothalamic amenorrhea. Journal of Clinical Endocrinology and Metabolism 64:1334, 1987.

Wilkinson, M., R. Bhanot and J.R. Brawer. Prolonged estrogen treatment induces changes in opiate benzodiazepine and beta-adrenergic binding sites in female rat hypothalamus. Brain Research Bulletin 11:279, 1983.

Wilkinson, M., R. Bhanot, D. Wilkinson and J.R. Brawer. Prolonged estrogen treatment induces chances in opiate, benzodiazepine and beta-adrenergic binding sites in female rat hypothalamus. Brain Research Bulletin 11:279, 1983.

Wilkinson, M., J.R. Brawer and D. Wilkinson. Gonadal steroid-induced modification of opiate binding sites in anterior hypothalamus of female rats. Biology of Reproduction 32:501, 1985.

Yen, S.S.C. The polycystic ovary syndrome. Clinical Endocrinology 12:177, 1980.

Zeleznik, A.J., A.R. Midgley and L.E. Reichert. Granulosa cell maturation in the rat: increased binding of human chorionic gonadotropin following treatment with follicle stimulating hormone *in vivo*. Endocrinology 95:818, 1974.

FIGURE 1 Light micrograph of a polycystic ovary 56 days after EV-injection. There are no corpora lutea and few secondary follicles. Precystic (pc) and cystic (C) follicles are a prominent feature of these ovaries.

x13.5

FIGURE 2 Light micrograph of a Type III Large Follicular Structure (III) from an EV-induced polycystic ovary, next to a macrocystic follicle (C). Note the large size of this structure relative to the cystic follicle, and the differences in the structure of the membrana granulosa and thecal wreaths.

x90

FIGURE 3 Light micrograph of an EV injected polycystic ovary. Three interstitial cell clusters (c) are labelled. A portion of a cyst wall can be seen at the top of the field.

x90

FIGURE 4 Light micrograph of an E_2-induced polycystic ovary. Clusters of secondary interstitial cells, engorged with lipid, are particularly abundant in these ovaries. Several clusters are located in the upper left-hand side of the field. The size of the microcystic follicle (c) present in this field can be compared to the macrocystic follicle in figure 2, photographed at the same magnification.

x90

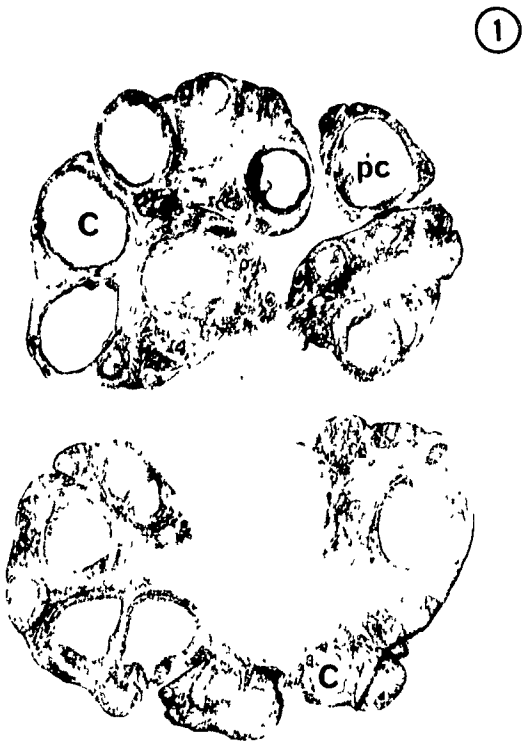
1
pc
C
C

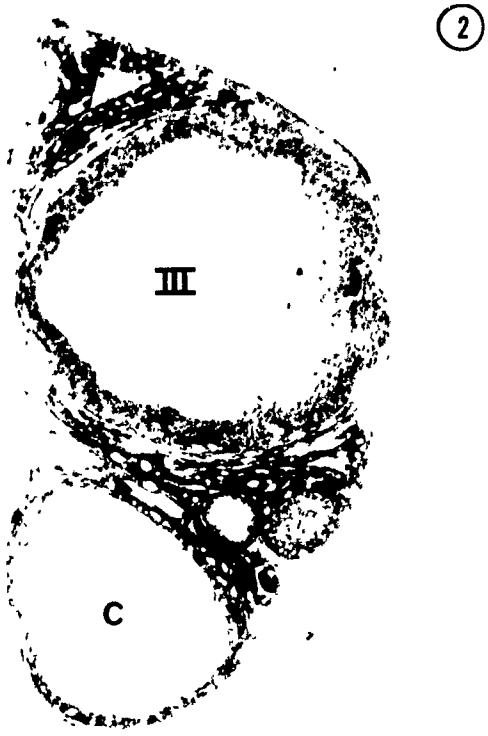
2
III
C


3
C
C
C

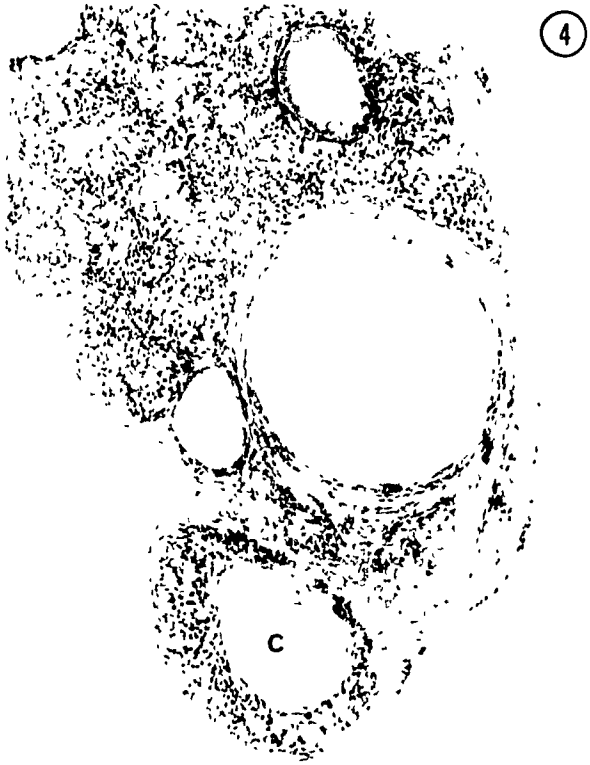
4
C

TABLE 1

Summary of the relative expression of alkaline phosphatase following immunostaining with biotinylated antibody against alkaline phosphatase in various cells of cystic and non-cystic ovaries.

In the rating scale used to index alkaline phosphatase expression, "0" denotes no activity, "±" an occasional positive reaction, "(+)" a weak reaction; "+" a consistent and definitive positive reaction, and "++" a strong reaction. Because vascular endothelial cells of the rat ovary show considerable alkaline phosphatase activity, an asterisk is used to signify when at least part of the reaction observed for a particular structure is given by blood vessels.

TABLE 1

Relative Expression of Alkaline Phosphatase following Immunostaining with Biotinylated Antibody against Alkaline Phosphatase in various cells of cystic and non-cystic ovaries

FOLLICLE AND CELL TYPE	CONTROL OVARIES	EV-TREATED OVARIES	E_2-IMPLANTED OVARIES
PRIMORDIAL/PRIMARY			
-granulosa	-	-	-
-thecal	(+)	(+)	(+)
SECONDARY/GRAAFIAN			
-granulosa	-	-	-
-thecal	++*	++*	++*
ATRETIC			
-granulosa	-	-	-
-thecal	++*	++*	++*
PRECYSTIC			
-granulosa	N/A	-	N/A
-thecal	N/A	++*	N/A
CYSTIC			
-granulosa	N/A	-	-
-thecal	N/A	(+)*	(+)*
SECONDARY INTERSTITIAL CELLS	+*	(±)*	(±) and ++*

FIGURE 5 Light micrograph of a control ovary stained for alkaline phosphatase (AP). Immunostain reaction product appears black in these micrographs. AP activity in stromal cells of primordial follicles (arrow) is weak compared to AP activity in primary (small arrowhead) and secondary (large arrowhead) follicular theca.

x225

FIGURE 6 Light micrograph of a control ovary stained for AP, illustrating relative intensities of AP activity in ovarian structures. AP activity is most pronounced in secondary follicular theca (h).

x13.5

FIGURE 7 Light micrograph of thecal cell layer from a secondary follicle (h) and a microcystic follicle (c) stained for AP. Endothelial cells are indicated by arrows. Note the major difference in thecal cell staining between the cyst and secondary follicle.

x225

FIGURE 8 Light micrograph of a control ovary stained for AP. The thecal reaction of healthy antral follicles (h) to AP immunostain is comparable to the thecal reaction of atretic antral follicles (a).

x36

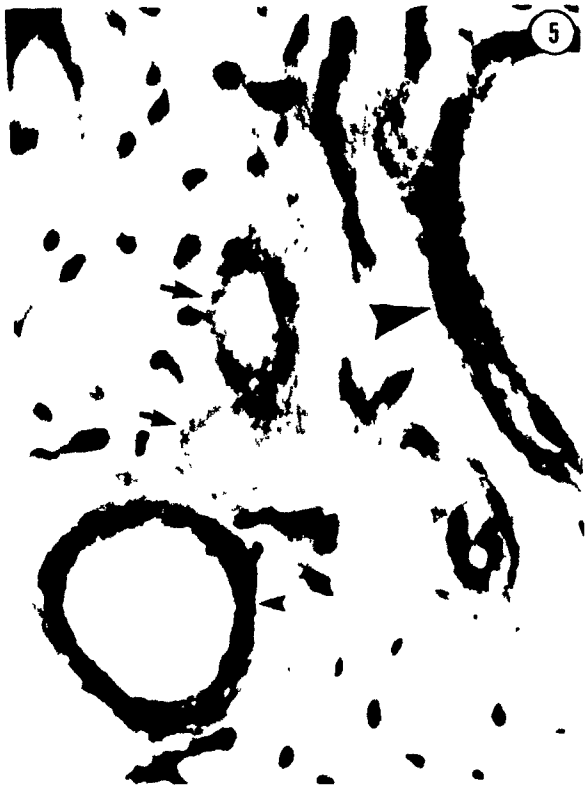

5

6

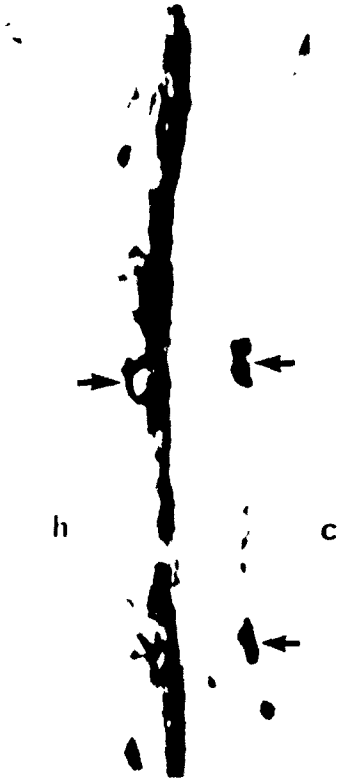

7

8

FIGURE 9 Light micrograph showing a secondary interstitial cell cluster from a control ovary immunostained for AP (area demarcated by arrows). These cells show a weak reaction to the immunostain, in contrast to the reaction of follicular thecal cells (large arrowheads) and vascular endothelial cells (small arrowheads).

x468

FIGURE 10 Light micrograph of AP-positive secondary interstitial cell strands (arrowheads) and a secondary interstitial cell cluster (arrow) from a microcystic ovary. The AP positive structure at the top of the field represents thecal cells encircling a primary follicle.

x360

FIGURE 11 Light micrograph from a macrocystic ovary immunostained for AP. The highly reactive thecal cell layer on the bottom (h) belongs to a healthy secondary follicle, in contrast to the moderately reactive one on the top which encircles a precystic follicle (pc).

x337.5

FIGURE 12 Light micrograph of the thecal cell layer of a healthy secondary follicle (h) and of a microcyst (c), immunostained for AP. The reaction in the microcystic thecal layer is primarily over endothelial cells, whereas both thecal and endothelial cells (arrowheads) in a secondary follicle are AP positive.

x540


9

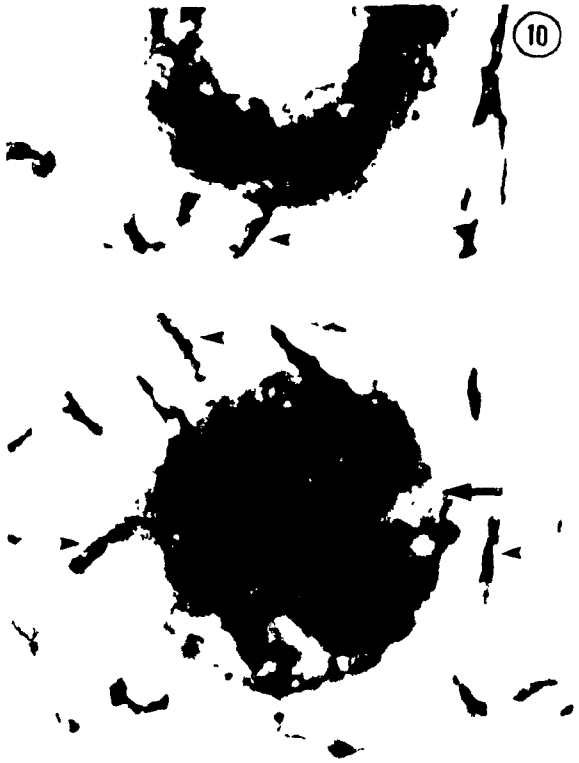
10


11
pc
h

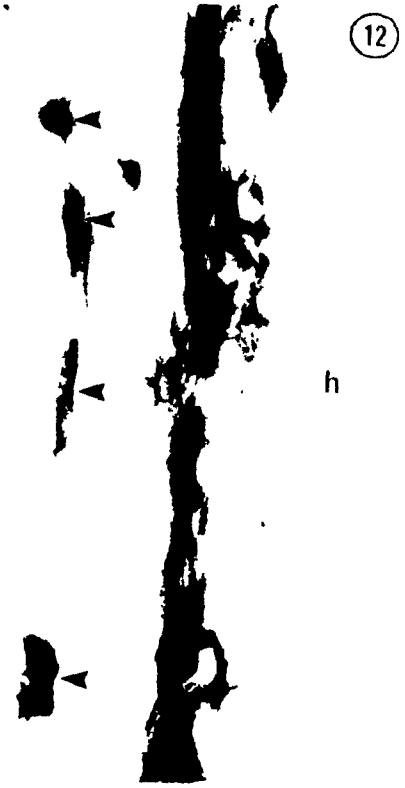
12
C
h

FIGURE 13 Mean Cell Size of Thecal and Secondary Interstitial Cells in an EV-Treated (Macrocystic) Ovary

This histogram represents the mean size of cells (n=20) from macrocystic ovaries ± standard error of the mean (S.E.M.). Healthy secondary thecal cells are significantly smaller than the other four cell types presented ($p<.001$). Macrocystic thecal cells are significantly larger than precystic follicular thecal cells ($p<.05$).

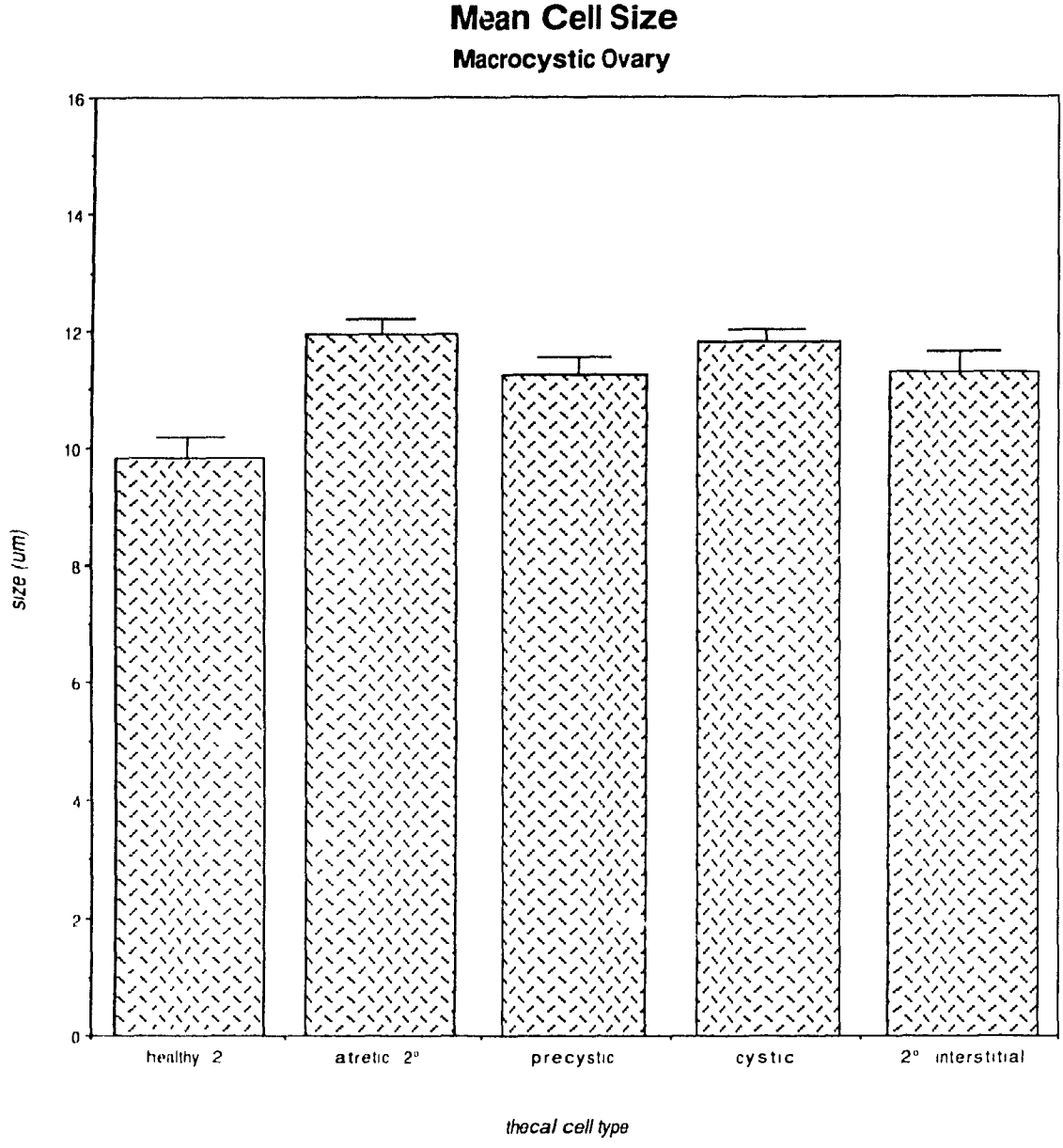
Mean Cell Size
Macrocystic Ovary
size (um)
16
14
12
10
8
6
4
2
0
healthy 2
atretic 2°
precystic
cystic
2° interstitial
thecal cell type

FIGURE 14 Electron micrograph of the membrana granulosa of a precystic follicle in a macrocystic ovary. Note the variability in cell and nuclear shape. Cytoplasmic blebbing of the apical surfaces is prominent on those cells in the right side of the field. Lipid droplets (L) and autophagic vacuoles (a), characteristic of a follicle in an advanced state of atresia, are labelled for reference. Luminal surface is at the top of the field.

x3,000

FIGURE 15 Electron micrograph of the membrana granulosa of a macrocystic follicle. It consists of a single layer of cells characterized by highly indented nuclei and large, irregular intercellular spaces. Luminal surface is at the top of the field.

x3,500

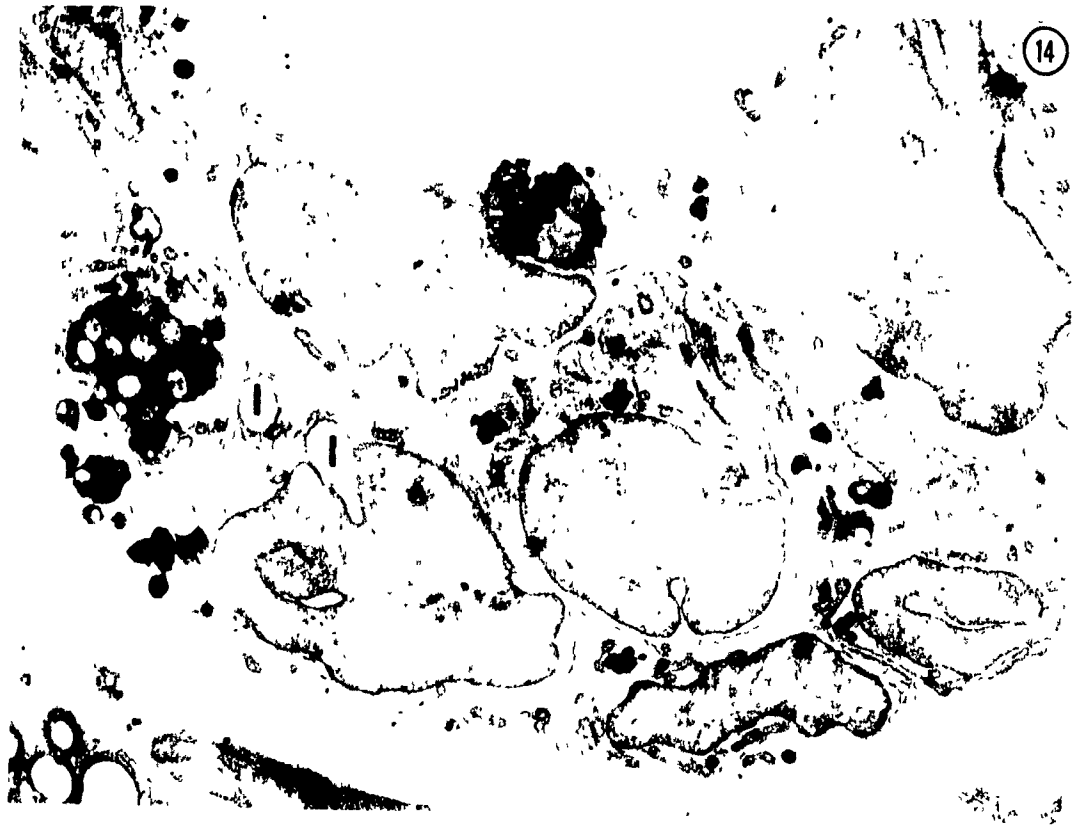

(14)

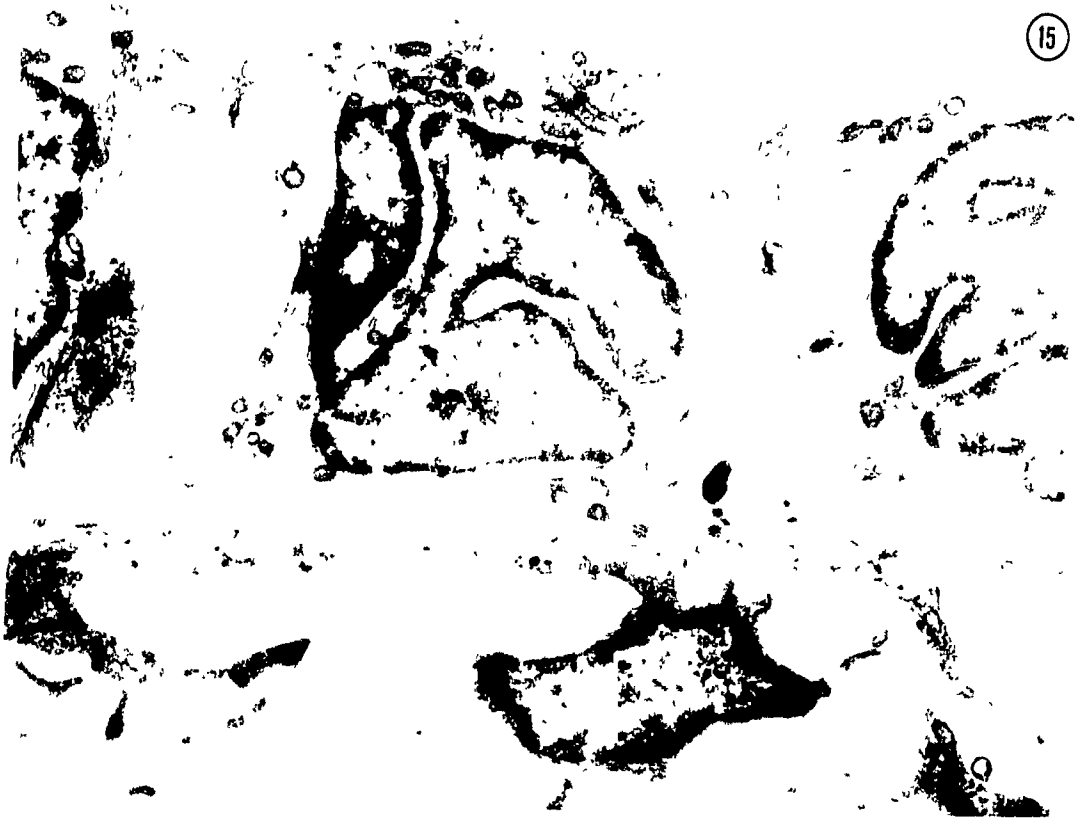

(15)

FIGURE 16 Electron microscopic radioautograph of thecal cells from a healthy secondary follicle. Grains represent binding of ^{125}I-hCG to LH/hCG receptors. Lipid appears as empty spheroidal inclusions.

x13,500


16

FIGURE 17 Electron microscopic radioautograph of a thecal cell from an atretic secondary follicle, photographed at the same magnification as Figure 16. In general, this cell is larger and more irregular in shape than healthy secondary follicular thecal cells. Its ultrastructural characteristics are similar.

x13,500

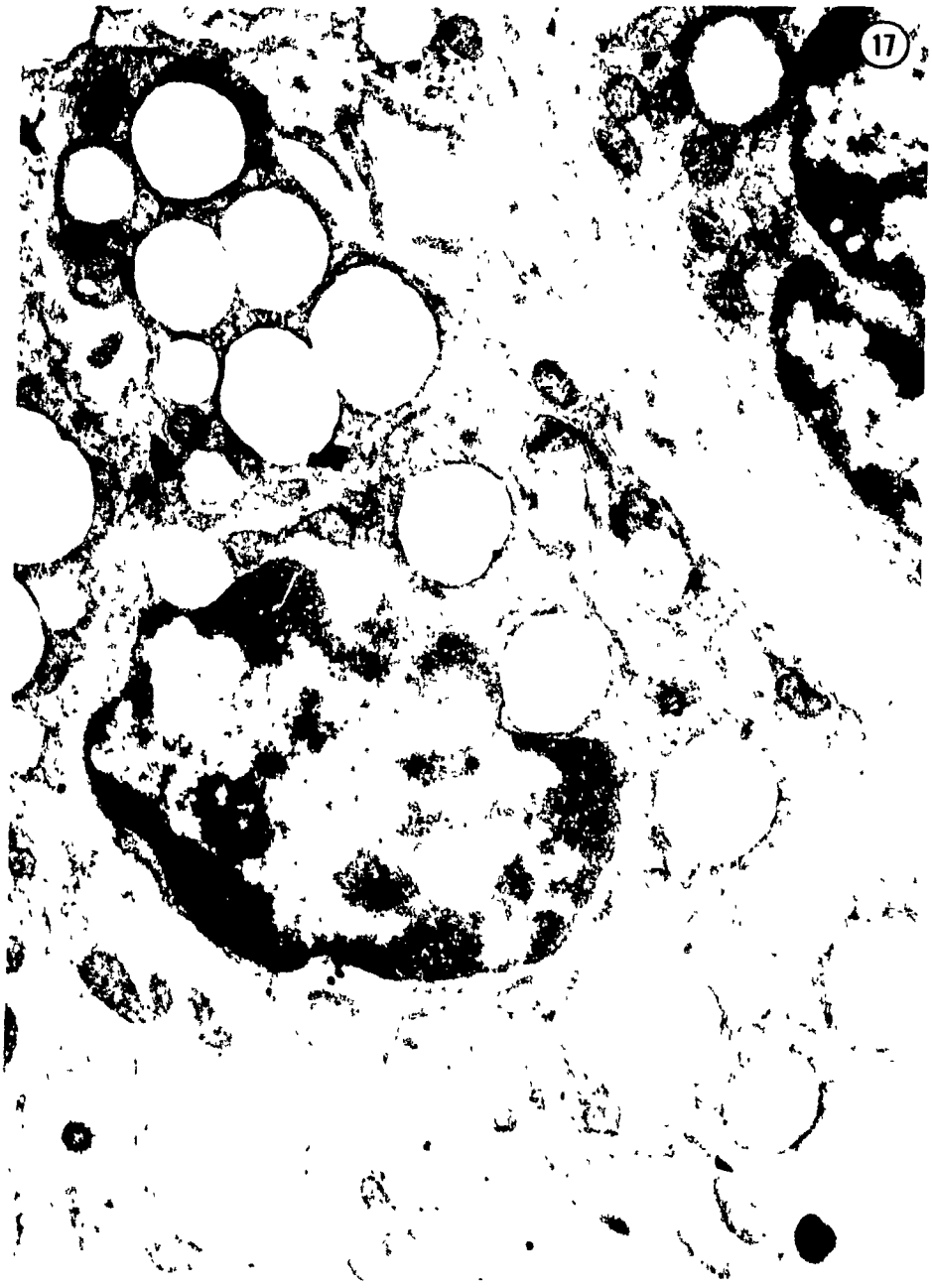
17

FIGURE 18a Electron microscopic radioautograph of a thecal cell from a precystic follicle (EV-treated ovary). The lipid droplets in these cells are significantly smaller than those within atretic and cystic thecal cells. Note the euchromatic state of the nucleus.

x12,600

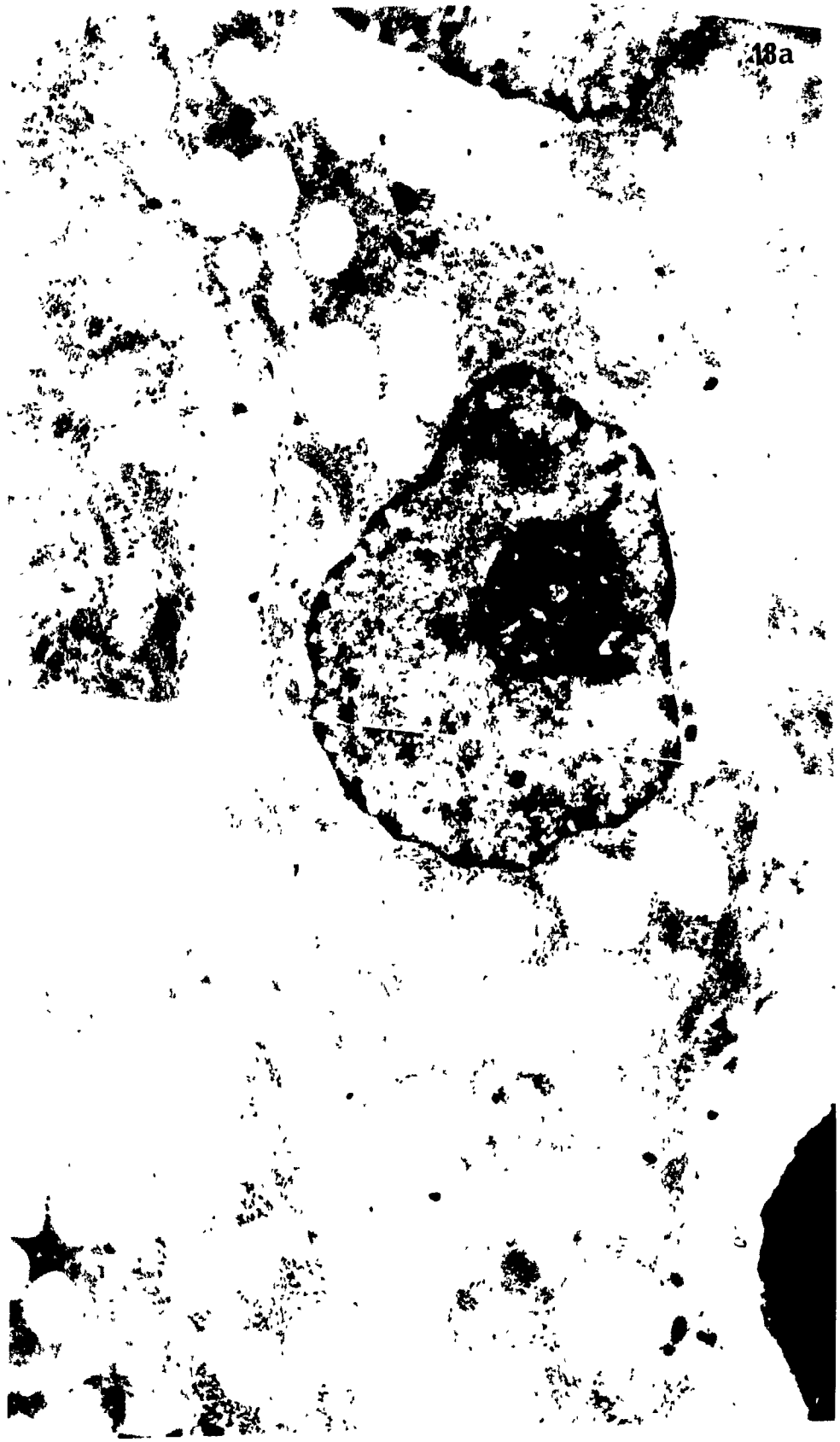
18a

FIGURE 18b Electron microscopic radioautograph of a thecal cell from a macrocystic follicle. These cells are significantly larger than precystic thecal cells. These cells contain the largest lipid droplets. This cell was located near the basal lamina of the cystic follicle and is, consequently a smaller representative macrocystic thecal cell. Note the heterochromatic state of the nucleus.

x12,600

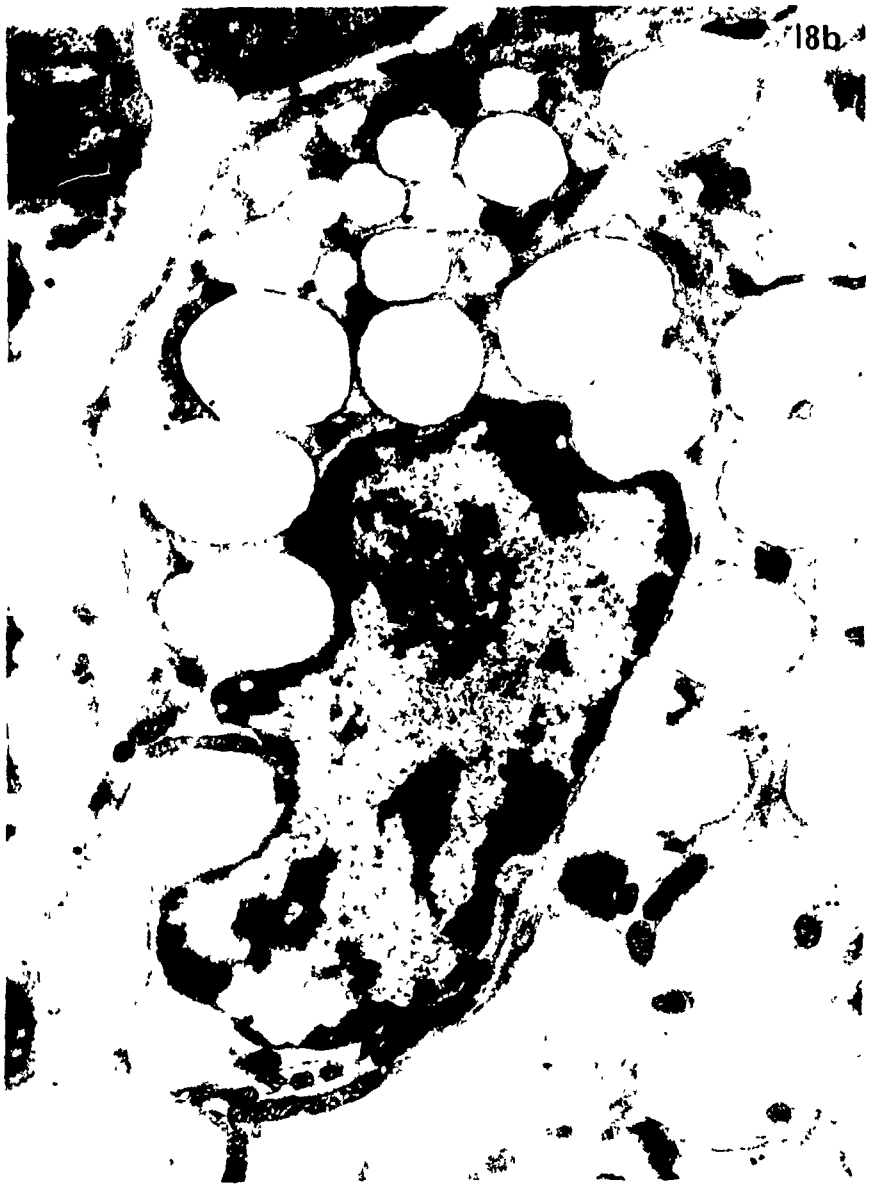
18b

FIGURE 19 Electron microscopic radioautograph of a secondary interstitial cell from a macrocystic ovary. These polygonally shaped cells are very large and give off numerous cytoplasmic projections. They contain an abundance of lipid droplets of a wide variety of sizes, and mitochondria with tubulovesicular cristae. Note the euchromatic state of the nucleus.

x12,600

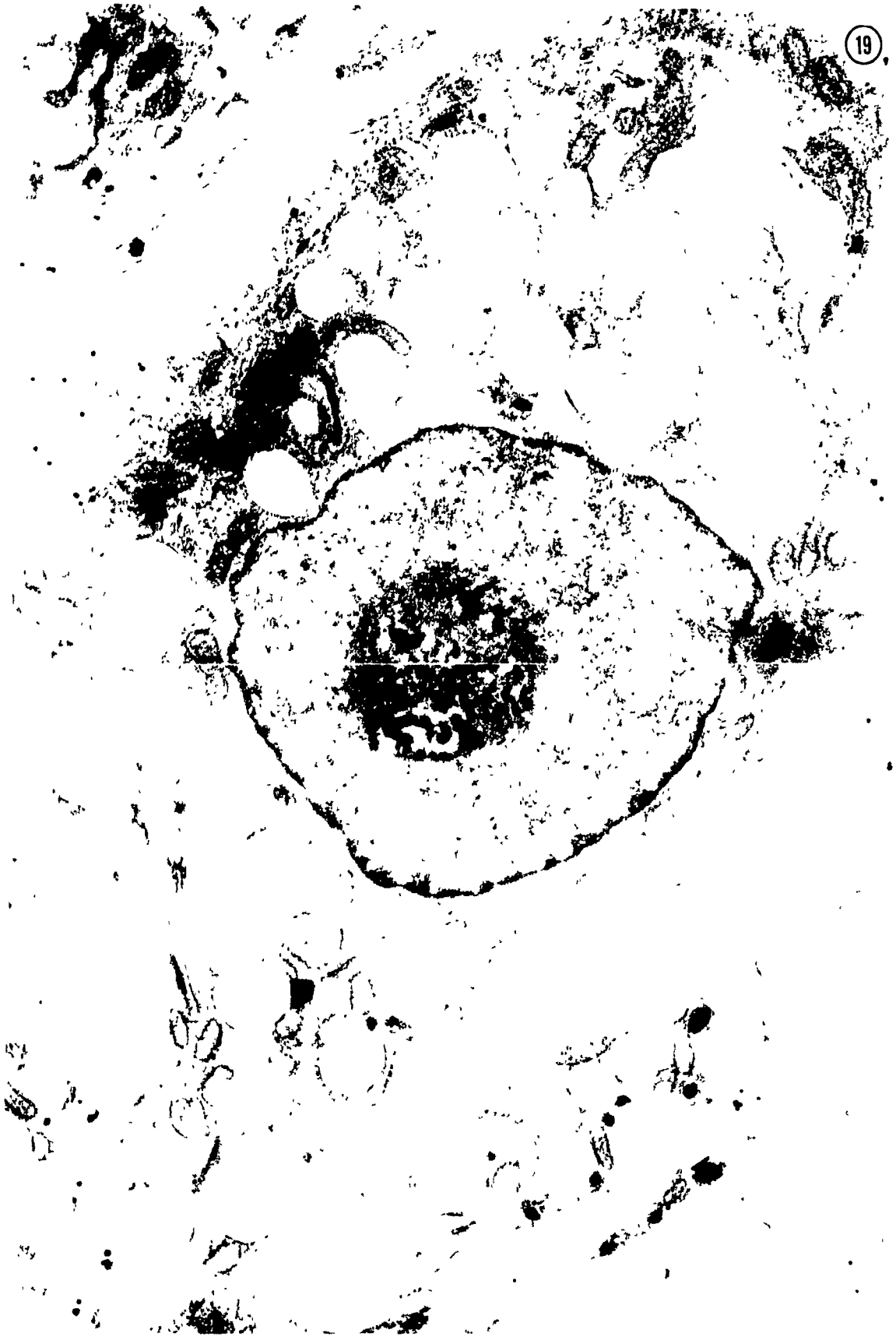
19

FIGURE 20 Mean Area of Lipid Droplets in Thecal and Secondary Interstitial Cells in a Macrocystic Ovary

This histogram represents the mean area of lipid droplets ± S.E.M. The mean area of lipid droplets within thecal cells of atretic secondary follicles is significantly larger than the mean lipid droplet area of healthy and precystic follicular thecal cells and secondary interstitial cells ($p<.002$). Lipid droplets within macrocystic thecal cells are significantly larger than those within the other four classes of cells studied ($p<.05$). There are no significant differences in the percentage of cell profile area occupied by lipid in these five different cell types. (n=10 cells/type).

Mean Lipid Droplet Area

Macrocystic Ovary

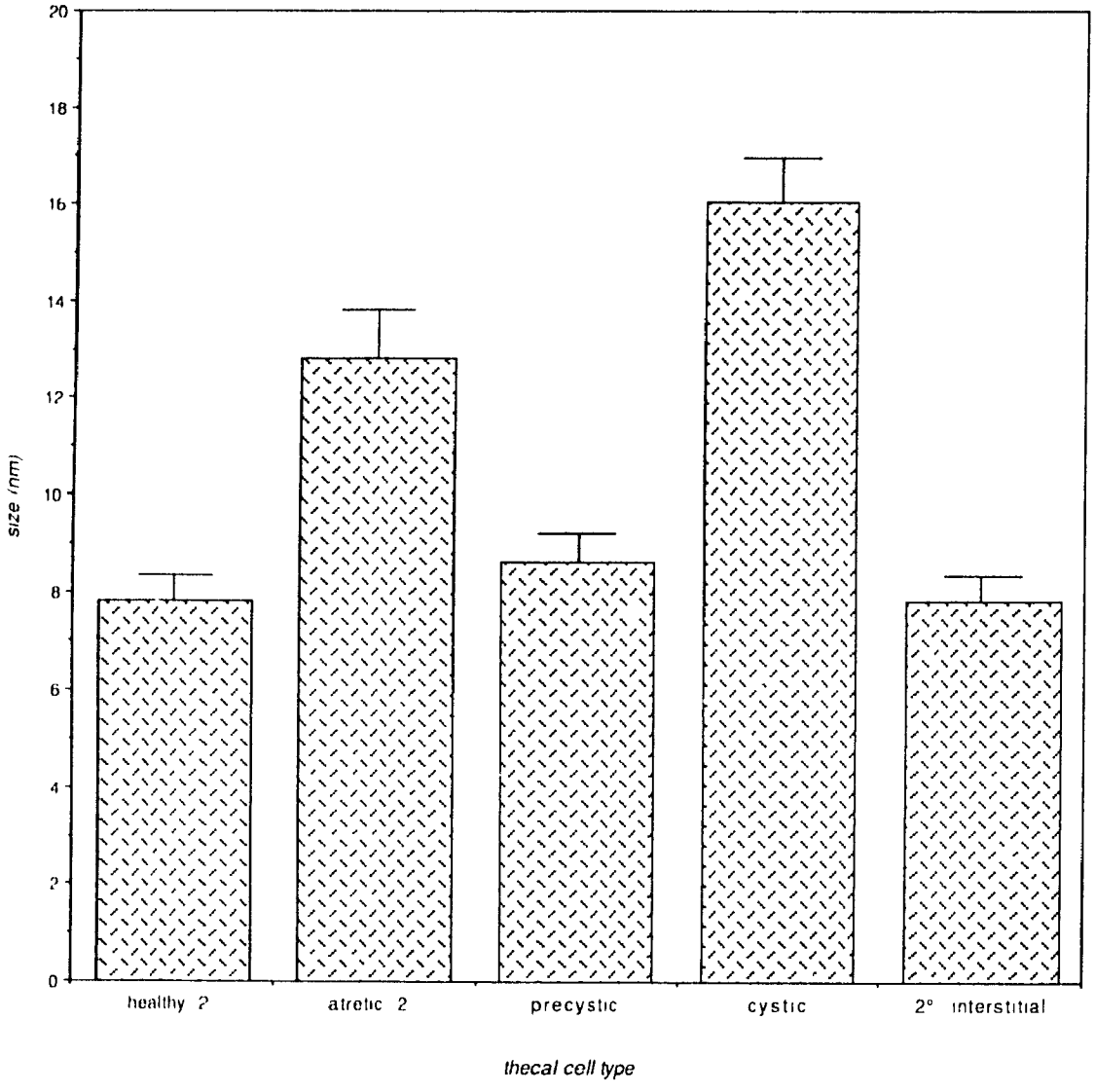

FIGURE 21 Mean Area of Mitochondrial Profiles in Thecal and Secondary Interstitial Cells in a Macrocystic Ovary

This histogram represents the mean area of mitochondrial profiles ± S.E.M. Mitochondrial profiles within atretic secondary follicular thecal cells are significantly smaller than those within thecal cells of healthy secondary, precystic and cystic follicular origin ($p<.05$). As well, the percentage of the atretic thecal cell profile area occupied by mitochondrial profiles is also significantly smaller than in healthy secondary and precystic thecal cells and secondary interstitial cells. Other differences are not significant. (n=10 cells/type).

Mean Mitochondrial Area

Macrocystic Ovary

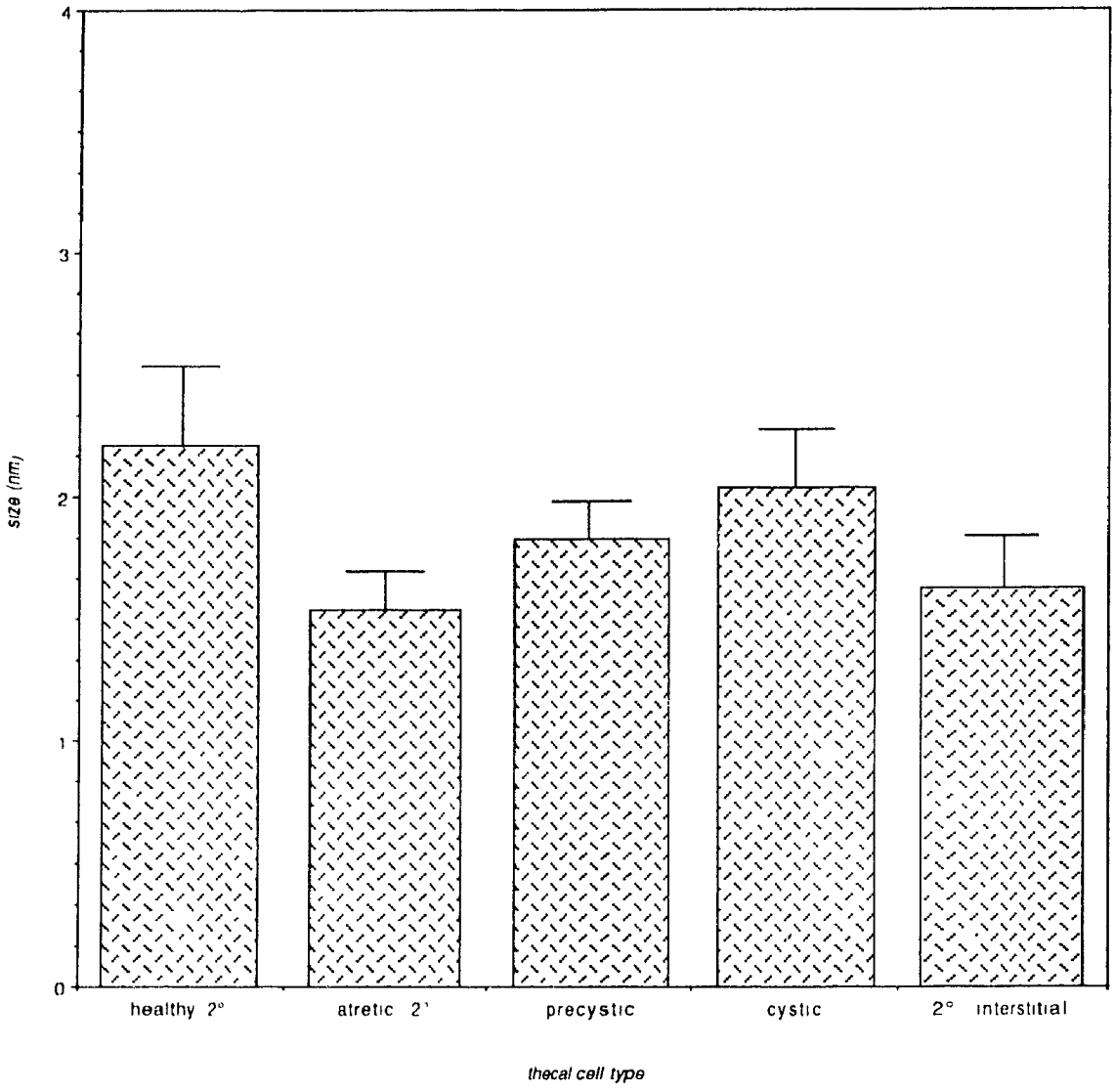

FIGURE 22 **Analysis of LH/hCG Binding Sites on Thecal and Secondary Interstitial Cells in a Macrocystic Ovary Using Electron Microscopic Radioautography**

Summary of the number of ^{125}I-hCG positive sites/1,000Ìm surface length on electron microscopic radioautographs. Differences in the mean number of grains/1000Ìm between healthy and atretic secondary follicular thecal cells are not significant. Precystic thecal cells possess significantly fewer binding sites than healthy and atretic follicular thecal cells ($p<.005$). Cystic thecal cells possess significantly fewer binding sites than all five cell types ($p<.001$). The mean number of grains associated with secondary interstitial cells is significantly greater than the number associated with atretic, precystic and cystic thecal cells ($p<.006$), but is not significantly different than the number of sites associated with thecal cells of healthy secondary follicles. (n=10 cells/type).

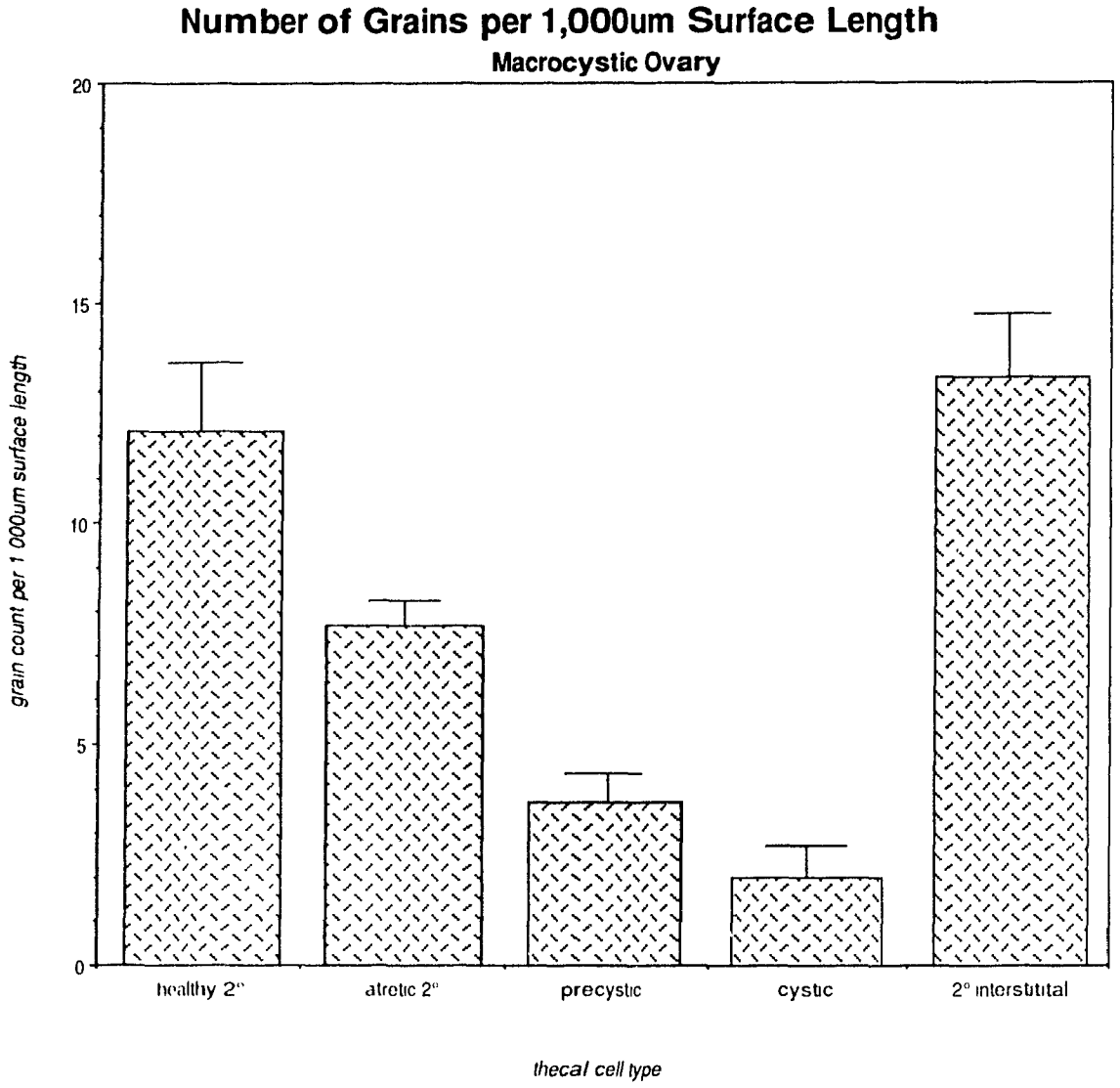
Number of Grains per 1,000um Surface Length
Macrocystic Ovary
grain count per 1 000um surface length
20
15
10
5
0
healthy 2°
atretic 2°
precystic
cystic
2° interstitial
thecal cell type

FIGURE 23 Mean Cell Size of Thecal and Secondary Interstitial Cells in E_2-Implanted (Microcystic) Ovaries

This histogram represents the mean size of cells (n=20) from microcystic ovaries $\pm$ S.E.M.. Atretic secondary follicular thecal cells are significantly larger than those of a healthy secondary follicle ($p<.001$). Secondary interstitial cell size is significantly larger than healthy and atretic follicular thecal cell size ($p<.05$).

Mean Cell Size

Microcystic Ovary

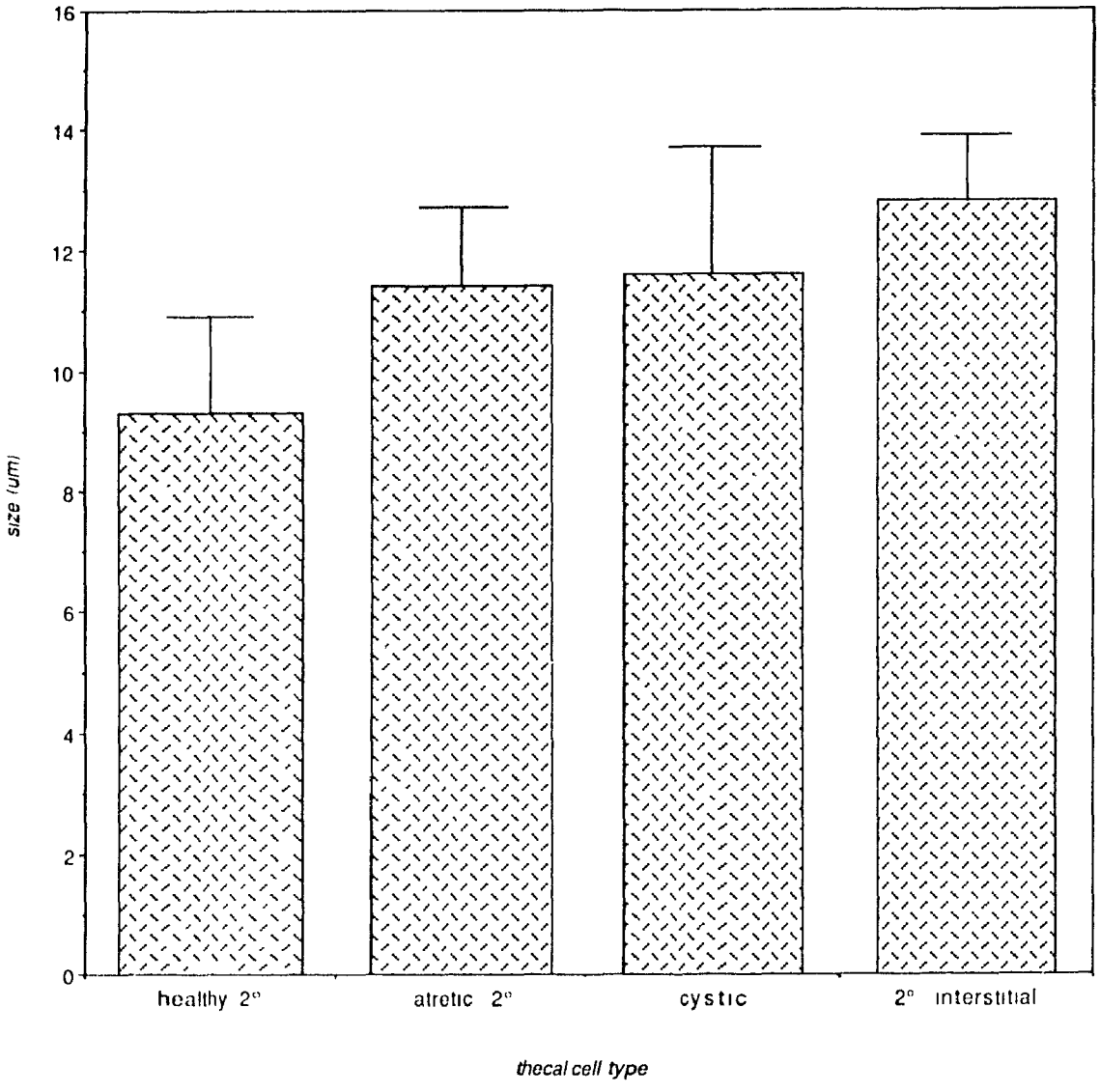

FIGURE 24 Electron micrograph of the membrana granulosa of a microcystic follicle, which possesses characteristics of the membrana granulosa of both precystic and cystic follicles in an EV-treated (macrocystic) polycystic ovary. Cells are irregularly shaped, give off numerous cytoplasmic extensions, and are held together by only a few remnant junctional complexes. Autophagic vacuoles are occasionally seen (upper right of field), while lipid droplets are not. A segment of basement membrane appears in the lower left corner of the field.

X5,300

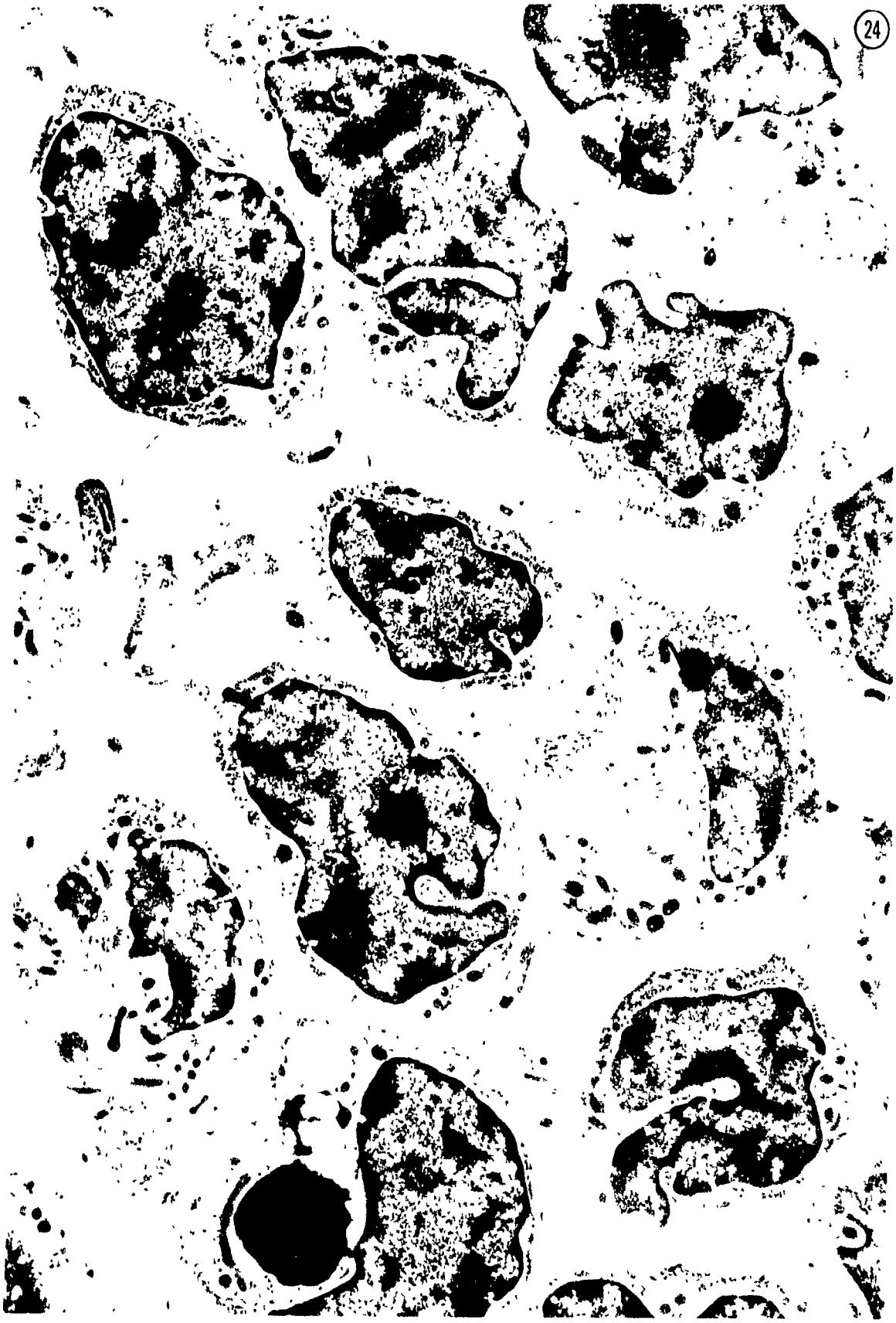

FIGURE 25 Electron microscopic radioautograph of a thecal cell from a microcystic follicle. These cells are approximately the same size as atretic secondary follicular thecal cells. The size of lipid droplets in these cells is significantly larger than healthy and atretic follicular thecal and secondary interstitial cell lipid droplets. Like macrocystic thecal cells, these cells possess very few LH binding sites. Note the heterochromatic state of the nucleus.

x12,600

FIGURE 26 Electron microscopic radioautograph of a secondary interstitial cell from a microcystic ovary. This cell is very similar morphologically to its counterpart in a macrocystic ovary, containing an abundance of lipid droplets of a wide variety of sizes, and mitochondria with tubulovesicular cristae. These cells contain significantly more LH/hCG binding sites than any other thecal cell type in a microcystic ovary, and appear to bind ^{125}I-hCG more extensively than macrocystic secondary interstitial cells. Note the euchromatic state of the nucleus.

x12,600

(26)

FIGURE 27 Mean Area of Lipid Droplets in Thecal and Secondary Interstitial Cells from a Microcystic Ovary

This histogram represents the mean area of lipid droplets ± S.E.M. There are no significant differences between mean area of lipid droplets within healthy and atretic secondary follicular or secondary interstitial cells. The mean lipid droplet area of cystic thecal cells is significantly larger than the other three cell types under study in these ovaries ($p<.007$). ($n=10$ cells/type).

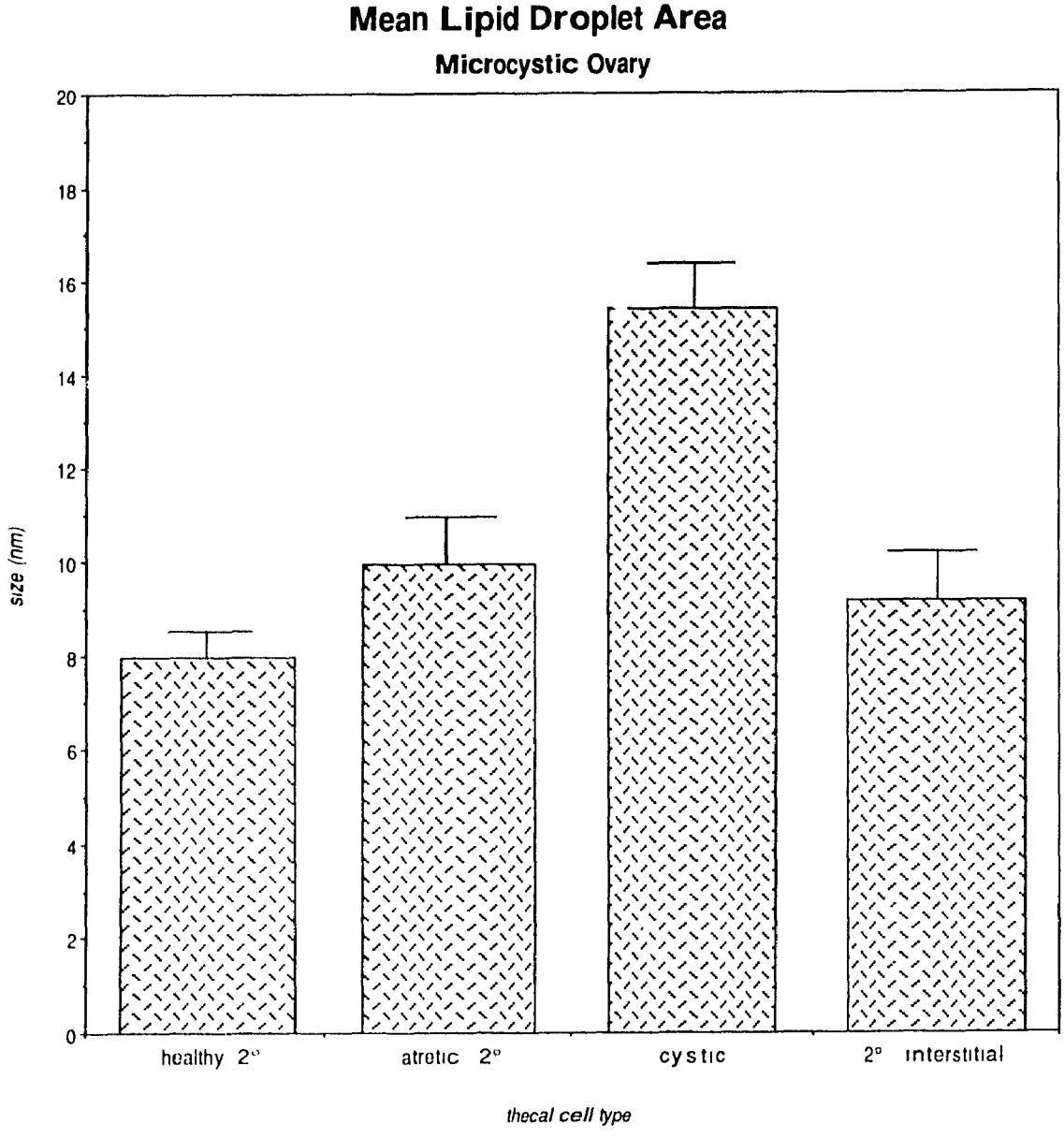
Mean Lipid Droplet Area
Microcystic Ovary
size (nm)
20
18
16
14
12
10
8
6
4
2
0
healthy 2°
atretic 2°
cystic
2° interstitial
thecal cell type

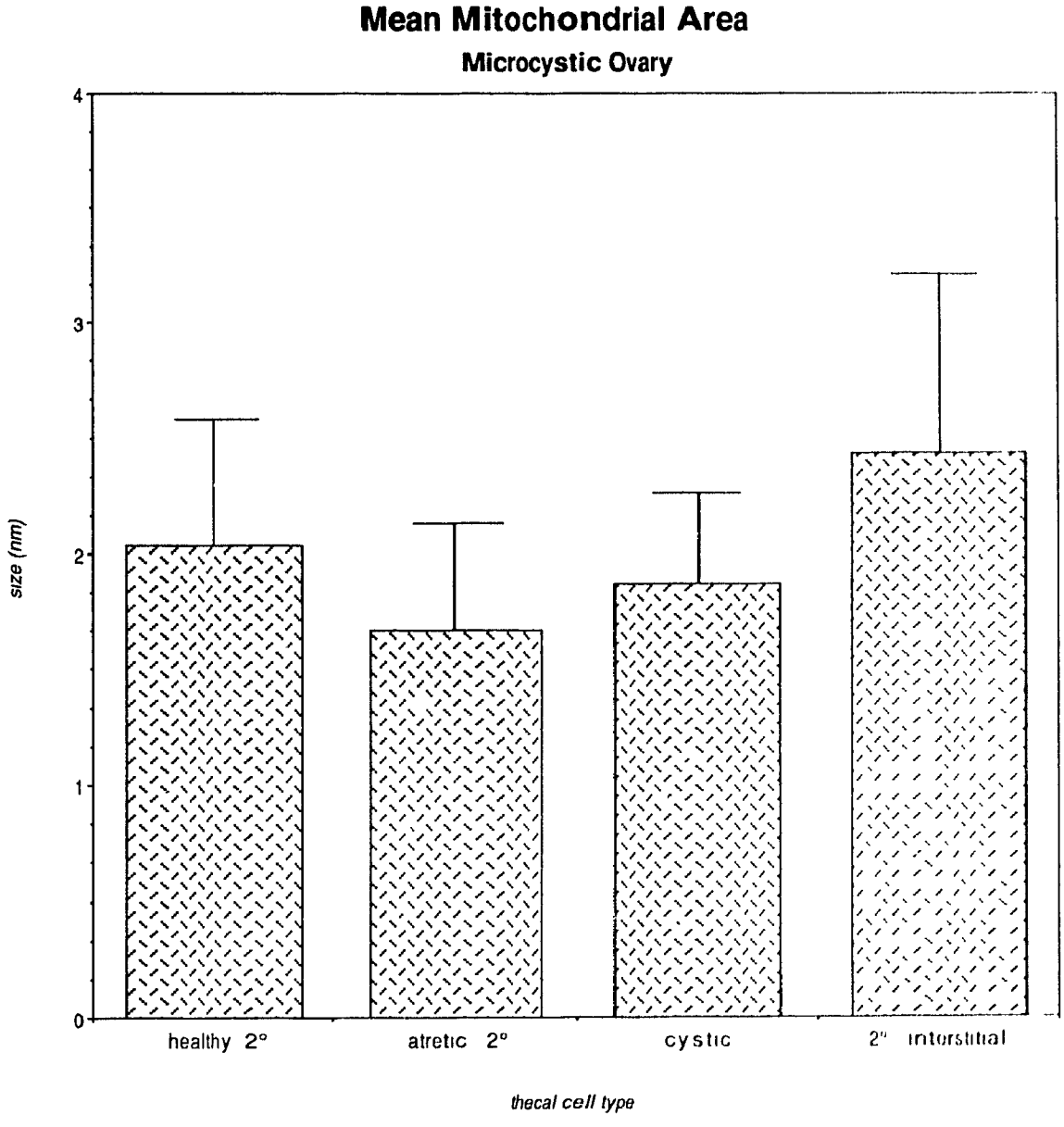
Mean Mitochondrial Area
Microcystic Ovary
size (nm)
4
3
2
1
0
healthy 2°
atretic 2°
cystic
2° interstitial
thecal cell type

FIGURE 28 Mean Area of Mitochondrial Profiles in Thecal and Secondary Interstitial Cells in Microcystic Ovaries

This histogram represents the mean area of mitochondrial profiles ± S.E.M. The mean area of mitochondrial profiles within secondary interstitial cells is significantly larger than mitochondrial profiles of atretic and cystic follicular origin ($p<.04$). There are no significant differences between the proportion of the total cell profile area occupied by mitochondrial profiles in these four cell types, however. (n=10 cells/type).

FIGURE 29 Analysis of LH/hCG Binding Sites on Thecal and Secondary Interstitial Cells in a Microcystic Ovary Using Electron Microscopic Radioautography

Summary of the number of ^{125}I-hCG binding sites/1,000Ìm surface length on electron microscopic radioautographs. Differences in the mean number of grains/1000Ìm between healthy and atretic secondary follicular thecal cells are not significant. Microcystic thecal cells possess significantly fewer LH binding sites than the other three cell types examined in these ovaries ($p<.001$). Secondary interstitial cells have a significantly larger number of LH receptors as compared to atretic secondary and microcystic thecal cells ($p<.004$). ($n=10$ cells/type).

Number of Grains per 1,000 um Surface Length

Microcystic Ovary